

# Double Coupled Canonical Polyadic Decomposition for Joint Blind Source Separation

Xiao-Feng Gong, *Member, IEEE*, Qiu-Hua Lin, *Member, IEEE*, Feng-Yu Cong, *Senior Member, IEEE*, and Lieven De Lathauwer, *Fellow, IEEE*

**Abstract** — Joint blind source separation (J-BSS) is an emerging data-driven technique for multi-set data-fusion. In this paper, J-BSS is addressed from a tensorial perspective. We show how, by using second-order multi-set statistics in J-BSS, a specific double coupled canonical polyadic decomposition (DC-CPD) problem can be formulated. We propose an algebraic DC-CPD algorithm based on a coupled rank-1 detection mapping. This algorithm converts a possibly underdetermined DC-CPD to a set of overdetermined CPDs. The latter can be solved algebraically via a generalized eigenvalue decomposition based scheme. Therefore, this algorithm is deterministic and returns the exact solution in the noiseless case. In the noisy case, it can be used to effectively initialize optimization based DC-CPD algorithms. In addition, we obtain the deterministic and generic uniqueness conditions for DC-CPD, which are shown to be more relaxed than their CPD counterparts. Experiment results are given to illustrate the superiority of DC-CPD over standard CPD with regards to uniqueness and accuracy.

**Index Terms** — Joint blind source separation, Tensor, Coupled canonical polyadic decomposition.

## I. INTRODUCTION

CANONICAL polyadic decomposition (CPD) decomposes a higher-order tensor into a minimal number of rank-1 terms. Compared with its matrix counterpart, CPD is essentially unique under mild conditions, without the need to exploit prior knowledge or impose particular constraints, and this nice identifiability property makes it a fundamental tool that is of particular interest for blind source separation (BSS). CPD has

Manuscript received XXXX XX, XXXX. This research is funded by: (1) National natural science foundation of China (nos. 61671106, 61331019, 61379012, 81471742); (2) Scientific Research Fund of Liaoning Education Department (no. L2014016); (3) Fundamental Research Funds for the Central Universities (nos. DUT16QY07). (4) China Scholarship Council; (5) Research Council KU Leuven: C1 project C16/15/059-nD. (6) FWO: project G.0830.14N, G.0881.14N; (7) the Belgian Federal Science Policy Office: IUAP P7/19 (DYSCO II, Dynamical systems, control and optimization, 2012-2017); (8) EU: The research leading to these results has received funding from the European Research Council under the European Union's Seventh Framework Programme (FP7/2007-2013) / ERC Advanced Grant: BIOTENSORS (no. 339804). This paper reflects only the authors' views and the Union is not liable for any use that may be made of the contained information.

Xiao-Feng Gong and Qiu-Hua Lin are with the School of Information and Communication Engineering, Dalian University of Technology, Dalian, China, 116024. (e-mails: xfgong@dlut.edu.cn, qhlin@dlut.edu.cn).

Feng-Yu Cong is with the Department of Biomedical Engineering, Dalian University of Technology, Dalian, China, 116024 (e-mail: cong@dlut.edu.cn).

Lieven De Lathauwer is with the STADIUS Center for Dynamical Systems, Signal Processing and Data Analytics; Department of Electrical Engineering (ESAT), KU Leuven, BE-3001 Leuven, Belgium; and Group Science, Engineering and Technology, KU Leuven, Kulak 8500 Kortrijk, Belgium (e-mail: Lieven.DeLathauwer@kuleuven.be).

indeed been successfully adopted in many BSS applications [1]–[8] including telecommunications, array signal processing, speech separation, and biomedical data analysis. Numerous CPD algorithms have been proposed in the literature [9]–[16], and its identifiability has been extensively studied, including its ability to deal with underdetermined BSS problems [6], [10]–[13], [17]–[22]. The incorporation of various constraints (e.g. nonnegativity, source independence, Vandermonde structure etc.) has also been investigated [23]–[28], aiming at improved performance in a variety of applications.

Recently, joint BSS (J-BSS) of multi-set signals has been considered in a number of applications such as multi-subject / multi-modal biomedical data fusion and BSS of transformed signals at multiple frequency bins for convolutive mixtures. These approaches usually assume dependence across datasets (inter-set dependence) and independence of latent sources within a dataset (intra-set independence), aiming at BSS of each individual dataset as well as indication of correspondences among decomposed components. A number of J-BSS algorithms have been proposed, e.g. joint and parallel independent component analysis (ICA) [29], independent vector analysis (IVA) [30]–[32], multi-set canonical correlation analysis (M-CCA) [33]–[35] and generalized joint diagonalization (GJD) [36]–[39]. We refer to [40] and references therein for an overview.

There are also tensor-based results that concern multi-set problems [41]–[59]. The concept of linked mode parallel factor analysis originated in [41]. Tensor probabilistic ICA (T-PICA) [42] has been extended and applied to multi-set fMRI via group T-PICA [43] and linked T-PICA [44], which assume shared source and shared mixing matrix, respectively. A simple case of coupled CPD (C-CPD) over two tensors has been discussed in [47]–[49] with applications to blind deconvolution of MIMO systems, joint EEG-MEG analysis, and array processing, respectively. Linked CPD with partially shared factors is addressed in [50]. A comprehensive study of uniqueness and an algebraic algorithm for the computation of C-CPD and coupled rank- $(L_{r,n}, L_{r,n}, 1)$  block term decomposition with one coupling factor matrix are provided in [51] and [52], respectively. Several applications of C-CPD in signal and array processing are discussed in [45], [46], [53]–[55]. Soft or flexible coupling has been considered as a way to deal with nonidentical but similar coupling factor matrices [56]–[58]. Recently, C-CPD with double coupling structure has been considered in [59].

However, the C-CPD approaches mentioned above are not specifically devised for J-BSS problems. More precisely, the

C-CPD approaches in [47]–[49] are limited to the case of two coupled tensor datasets. The approaches in [50]–[58] based on either hard or soft coupling structure are mainly used to fuse multiple datasets which have tensor form, while the general multi-set data formulation in J-BSS is in matrix form. The T-PICA variants [42]–[44] assume that either the mixing matrices or the sources for different datasets are the same, and thus may not work well in applications where this crucial assumption is not satisfied. In fact, as will be shown later, by using second-order statistics of the multi-set signal, we can obtain a set of tensors admitting a specific double coupled CPD (DC-CPD) formulation with coupling in two modes, possibly with a conjugation structure for complex-valued problems (an illustration is given in Fig. 1). The coupling factor matrices of this specific DC-CPD may not have full column rank. We note that the GJD formulation in [36]–[39] is similar to DC-CPD, but is limited to the case where the coupling factor matrices have full column rank. As such, to the best of our knowledge, the specific but important DC-CPD problem has not been thoroughly studied in the literature. It will be addressed in this paper, both from a theoretical and a practical perspective.

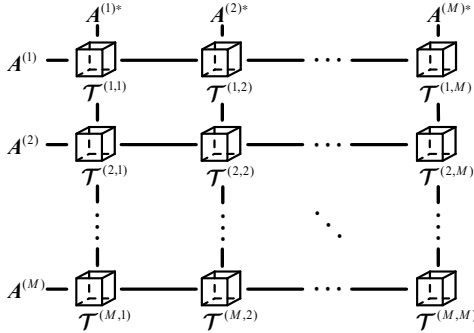


Fig. 1. Illustration of DC-CPD. The tensors are placed at different nodes of a grid according to their indices. The tensor at node  $(m, n)$  admits  $\mathcal{T}^{(m,n)} = \llbracket \mathbf{A}^{(m)}, \mathbf{A}^{(n)*}, \mathbf{C}^{(m,n)} \rrbracket_R$ ,  $m, n = 1, \dots, M$ . Tensors in the  $m$ th row of the grid are coupled in the first mode by  $\mathbf{A}^{(m)}$ . Tensors in the  $m$ th column of the grid are coupled in the second mode by  $\mathbf{A}^{(m)*}$ .

In Section II, we explain how second-order statistics can be used to formulate a DC-CPD from the matrix data in J-BSS. In Section III, we present an algebraic algorithm based on a new coupled rank-1 detection mapping. We will show that it is possible to compute an exact DC-CPD by means of conventional linear algebra, essentially by solving overdetermined sets of linear equations, low-rank matrix approximation and generalized eigenvalue decomposition (GEVD), **even in underdetermined cases where the number of sources exceeds the number of observations**. In addition, we obtain deterministic and generic uniqueness conditions for DC-CPD; **the two main results are Theorem 2 and its further generalization Theorem 3**. In Section IV, experiment results are provided to demonstrate the performance of DC-CPD, in comparison with CPD. Section V concludes this paper.

*Notation:* Vectors, matrices and tensors are denoted by lower-case boldface, uppercase boldface and uppercase calligraphic letters, respectively. The  $r$ th column vector and the  $(i, j)$ th entry of  $\mathbf{A}$  are denoted by  $\mathbf{a}_r$  and  $a_{ij}$ , respectively. The identity matrix, all-zero matrix and all-zero vectors are denoted by  $\mathbf{I}_M \in \mathbb{C}^{M \times M}$ ,

$\mathbf{0}_{M,N} \in \mathbb{C}^{M \times N}$ ,  $\mathbf{0}_M \in \mathbb{C}^M$ , respectively. The subscripts are omitted if there is no ambiguity. The null space of a matrix  $\mathbf{M}$  is denoted as  $\ker(\mathbf{M})$ . The dimensionality of a vector space  $\mathfrak{S}$  is denoted as  $\dim(\mathfrak{S})$ . Transpose, conjugate, conjugated transpose, Moore-Penrose pseudo-inverse, Frobenius norm and matrix determinant are denoted as  $(\cdot)^T$ ,  $(\cdot)^*$ ,  $(\cdot)^H$ ,  $(\cdot)^\dagger$ ,  $\|\cdot\|_F$ , and  $|\cdot|$ , respectively.

The symbols ‘ $\otimes$ ’, ‘ $*$ ’, ‘ $\odot$ ’ and ‘ $\circledast$ ’ denote Kronecker product, Hadamard product, Khatri-Rao product, and tensor outer product, respectively, defined as follows:

$$\mathbf{A} \otimes \mathbf{B} \triangleq \begin{bmatrix} a_{11}\mathbf{B} & a_{12}\mathbf{B} & \cdots \\ a_{21}\mathbf{B} & a_{22}\mathbf{B} & \cdots \\ \vdots & \vdots & \ddots \end{bmatrix}, \mathbf{A} * \mathbf{B} \triangleq \begin{bmatrix} a_{11}b_{11} & a_{12}b_{12} & \cdots \\ a_{21}b_{21} & a_{22}b_{22} & \cdots \\ \vdots & \vdots & \ddots \end{bmatrix},$$

$$\mathbf{A} \odot \mathbf{B} \triangleq [a_1 \otimes b_1, a_2 \otimes b_2, \dots], (\mathbf{a} \circledast \mathbf{b} \circledast \mathbf{c})_{i,j,k} \triangleq a_i b_j c_k.$$

We denote  $\odot_{u \in \Omega} \mathbf{B}^{(u)}$  and  $\otimes_{u \in \Omega} \mathbf{B}^{(u)}$  as the Khatri-Rao product and Kronecker product of all the matrices  $\mathbf{B}^{(u)}$  with  $u \in \Omega$ , respectively. Mathematical expectation is denoted as  $E\{\cdot\}$ . MATLAB notation will be used to denote submatrices of a tensor. For instance, we use  $(\mathcal{T})_{(\cdot,\cdot,k)}$  or  $\mathcal{T}_{(\cdot,\cdot,k)}$  to denote the frontal slice of tensor  $\mathcal{T}$  obtained by fixing the third index to  $k$ . A polyadic decomposition (PD) of  $\mathcal{T}$  expresses  $\mathcal{T}$  as the sum of rank-1 terms:

$$\mathcal{T} = \llbracket \mathbf{A}, \mathbf{B}, \mathbf{C} \rrbracket_R \triangleq \sum_{r=1}^R \mathbf{a}_r \circledast \mathbf{b}_r \circledast \mathbf{c}_r \in \mathbb{C}^{I \times J \times K}, \quad (1)$$

where  $\mathbf{A} \triangleq [\mathbf{a}_1, \dots, \mathbf{a}_R] \in \mathbb{C}^{I \times R}$ ,  $\mathbf{B} \triangleq [\mathbf{b}_1, \dots, \mathbf{b}_R] \in \mathbb{C}^{J \times R}$ , and  $\mathbf{C} \triangleq [\mathbf{c}_1, \dots, \mathbf{c}_R] \in \mathbb{C}^{K \times R}$ . We call (1) a canonical PD (CPD) if  $R$  is minimal.

For an  $N$ th-order tensor  $\mathcal{T} \in \mathbb{C}^{I_1 \times \dots \times I_N}$ ,  $\text{vec}(\mathcal{T}) \in \mathbb{C}^{I_1 \dots I_N}$  denotes the vector representation of  $\mathcal{T}$  defined by  $[\text{vec}(\mathcal{T})]_{\tilde{i}} \triangleq t_{i_1, \dots, i_N}$ , with  $\tilde{i} = \sum_{n=1}^N (i_n - 1) \prod_{m=1}^{N-n} I_m + 1$ , while  $\text{unvec}(\cdot)$  performs the inverse. The mode- $i$  matrix representation of a third-order tensor  $\mathcal{T} \in \mathbb{C}^{I \times J \times K}$  is denoted as  $\mathbf{T}_i$ ,  $i = 1, 2, 3$ , and defined by:

$$(\mathbf{T}_1)_{(j-1)K+k,i} = (\mathbf{T}_2)_{(i-1)K+k,j} = (\mathbf{T}_3)_{(i-1)J+j,k} = t_{i,j,k}.$$

We define  $\text{Ten}(\mathbf{T}, [I_1, \dots, I_{K-1}, J]) = \mathcal{T}$  as the operation to reshape a  $\prod_{k=1}^{K-1} I_k \times J$  matrix  $\mathbf{T}$  into a  $K$ th-order tensor  $\mathcal{T}$  of size  $I_1 \times \dots \times I_{K-1} \times J$ , such that:

$$t_{i_1, \dots, i_{K-1}, j} = (\mathbf{T})_{\tilde{i}, j}, \text{ where } \tilde{i} \triangleq \sum_{k=1}^{K-1} (i_k - 1) \prod_{m=1}^{K-k-1} I_m + 1.$$

The operator  $\text{perm}_p(\mathcal{T})$  permutes the index of  $\mathcal{T}$  according to a permutation vector  $\mathbf{p}$ . For instance,  $\text{perm}_{(2,1,3)}(\mathcal{T})$  permutes the first and second indices of  $\mathcal{T}$ . Concatenation of tensors  $\mathcal{T}_1 \in \mathbb{C}^{I \times J \times K_1}, \dots, \mathcal{T}_N \in \mathbb{C}^{I \times J \times K_N}$  in the last mode is denoted as  $\mathcal{T} \triangleq \text{cat}(\mathcal{T}_1, \dots, \mathcal{T}_N) \in \mathbb{C}^{I \times J \times (K_1 + \dots + K_N)}$ .

The number of  $k$ -permutations from a set of  $m$  elements is defined as  $P_m^k \triangleq m \cdot (m-1) \cdots (m-k+1)$ , and the number of  $k$ -combinations from a set of  $m$  elements is defined as  $C_m^k \triangleq P_m^k / k!$ . The cardinality of a set is denoted as  $\text{card}(\cdot)$ .

## II. PROBLEM FORMULATION

J-BSS usually assumes the following multi-set data model:

$$\mathbf{x}^{(m)}(t) = \mathbf{A}^{(m)} \mathbf{s}^{(m)}(t), \quad m = 1, \dots, M, \quad (2)$$

where  $\mathbf{x}^{(m)}(t) \in \mathbb{C}^N$ ,  $\mathbf{s}^{(m)}(t) \in \mathbb{C}^R$  denote the mixture and source at time instant  $t$ , respectively, and  $\mathbf{A}^{(m)} \in \mathbb{C}^{N \times R}$  is the mixing matrix for the  $m$ th dataset. In practice, there is also a noise term. Here we omit it for convenience.  $N$ ,  $R$  and  $M$  are the number of observations, sources, and datasets respectively. J-BSS aims at estimating the mixing matrices  $\mathbf{A}^{(m)}$  and/or sources  $\mathbf{s}^{(m)}(t)$  for  $m = 1, \dots, M$ . In particular, if only the mixing matrices are of interest, the problem is called joint blind identification (J-BI). We say a J-BSS is underdetermined if  $N < R$ , and is overdetermined if  $N \geq R$ .

With the multi-set data model (2), we additionally assume that  $s_r^{(m)}(t)$  and  $s_u^{(n)}(t)$  are independent for  $1 \leq r \neq u \leq R$  (intra-set independence) and dependent for  $1 \leq r = u \leq R$  (inter-set dependence), regardless of the value of  $m$  and  $n$ . The idea is now to obtain a set of tensors by stacking second-order cross-covariance matrices. We assume that the sources are temporally nonstationary with zero mean and unit variance. Then we obtain a set of cross-covariance tensors as:

$$\begin{aligned} (\mathcal{T}^{(m,n)})_{(:, :, t)} &= \mathbb{E} \{ \mathbf{x}^{(m)}(t) [\mathbf{x}^{(n)}(t)]^H \} \\ &= \mathbf{A}^{(m)} \mathbb{E} \{ \mathbf{s}^{(m)}(t) [\mathbf{s}^{(n)}(t)]^H \} \mathbf{A}^{(n)H}, \end{aligned} \quad (3)$$

where  $\mathcal{T}^{(m,n)} \in \mathbb{C}^{N \times N \times T}$ ,  $1 \leq m, n \leq M$ . We note that the frontal slice  $(\mathcal{T}^{(m,n)})_{(:, :, t)}$  is the cross-covariance matrix between the  $m$ th and  $n$ th datasets at time instant  $t$ , and that  $T$  denotes the number of time frames for which such a cross-covariance is computed. Observing that  $\mathbb{E} \{ \mathbf{s}^{(m)}(t) [\mathbf{s}^{(n)}(t)]^H \}$  is diagonal under the assumption of intra-set independence and inter-set dependence, we can rewrite (3) as follows:

$$\mathcal{T}^{(m,n)} = \sum_{r=1}^R \mathbf{a}_r^{(m)} \otimes \mathbf{a}_r^{(n)*} \otimes \mathbf{c}_r^{(m,n)} = \left[ \mathbf{A}^{(m)}, \mathbf{A}^{(n)*}, \mathbf{C}^{(m,n)} \right]_R, \quad (4)$$

where  $\mathbf{c}_r^{(m,n)}(t) = \mathbb{E} \{ s_r^{(m)}(t) [s_r^{(n)}(t)]^H \}$ , and  $\mathbf{C}^{(m,n)} \triangleq [\mathbf{c}_1^{(m,n)}, \dots, \mathbf{c}_R^{(m,n)}]$ . We see that for fixed  $m$  and  $n$ , (4) is by itself a PD. For varying  $m$  and  $n$ , each PD shares factor matrices with other PDs in the first two modes, which we denote as ‘‘double coupling’’. More precisely, if we place the tensors  $\mathcal{T}^{(m,n)}$  at different nodes of a grid according to their indices (see Fig. 1), we can see that all the tensors in the same ‘‘column’’ (e.g. the  $m$ th column) are coupled in the first mode (by  $\mathbf{A}^{(m)}$ ), and all the tensors in the same ‘‘row’’ (e.g. the  $n$ th row) are coupled in the second mode (by  $\mathbf{A}^{(n)*}$ ). For instance, for  $M = 3$  we note that  $\mathcal{T}^{(1,1)}$ ,  $\mathcal{T}^{(1,2)}$ , and  $\mathcal{T}^{(1,3)}$  are coupled in the first mode by factor matrix  $\mathbf{A}^{(1)}$ . Similarly,  $\mathcal{T}^{(1,3)}$ ,  $\mathcal{T}^{(2,3)}$ , and  $\mathcal{T}^{(3,3)}$  are coupled in the second mode by  $\mathbf{A}^{(3)*}$ . We define the set of rank-1 terms  $\{ \mathbf{a}_r^{(m)} \otimes \mathbf{a}_r^{(n)*} \otimes \mathbf{c}_r^{(m,n)}, m, n = 1, \dots, M \}$  as a double coupled rank-1 term, and the set of tensors  $\{ \mathcal{T}^{(m,n)}, m, n = 1, \dots, M \}$  is said to admit an  $R$ -term double coupled PD. If the number of double coupled rank-1 terms  $R$  in (4) is minimal, then the double coupled PD is denoted as double coupled canonical PD (DC-CPD). Our goal is to decompose the tensors  $\mathcal{T}^{(m,n)}$  into a minimal number of double coupled rank-1 terms, to recover the mixing matrices  $\mathbf{A}^{(m)}$ .

So far, we have shown how, via the computation of second-order statistics, the stochastic multi-set signals in (2) are trans-

formed into a set of tensors, the joint decomposition of which takes the form of a DC-CPD (4). This method fits in the tensorization framework proposed in [60]. In line with the discussion in [60], the inherent intra-set independence and inter-set dependence of sources are key in the conversion, and have in fact already been used in existing practical multi-set signal processing applications, not necessarily in the J-BSS framework *sensu stricto*. For example, for linear convolutive mixtures that are transformed to the frequency domain, the cross-correlations of components at neighboring frequency bins are intensively exploited to solve the permutation misalignment problem [30], [39], [47], [62]. The above assumptions on multi-set statistics are also used in group analysis of biomedical data [29], [31]–[39] where the multiple datasets may refer to data of multiple modalities (e.g. fMRI, MEG, EEG) collected from a single subject under equal conditions, or data collected from multiple subjects, possibly using a single modality but acquired under the same conditions.

*Remark 1:* Note that the DC-CPD (4) derived from (3) has a conjugated symmetric structure:  $\mathcal{T}^{(m,n)} = \text{perm}_{(2,1,3)}(\mathcal{T}^{(n,m)*})$ . In cases where this symmetry is not readily present, we are able to create it by tensor concatenation. Let us denote the tensors in an asymmetric DC-CPD as  $\mathcal{T}^{(m,n)} = \left[ \mathbf{A}^{(m)}, \mathbf{A}^{(n)*}, \mathbf{C}^{(m,n)} \right]_R$ , and group these tensors into  $M$  sets  $\Upsilon^{(1)}, \dots, \Upsilon^{(M)}$ . Each set  $\Upsilon^{(m)}$  contains  $2M$  tensors that have a common factor matrix  $\mathbf{A}^{(m)}$ , for fixed  $m$ :

$$\Upsilon^{(m)} \triangleq \{ \mathcal{T}^{(m,1)}, \text{perm}_{(2,1,3)}(\mathcal{T}^{(1,m)*}), \dots, \mathcal{T}^{(m,M)}, \text{perm}_{(2,1,3)}(\mathcal{T}^{(M,m)*}) \}. \quad (5)$$

The  $2M$  tensors in  $\Upsilon^{(m)}$  can be further grouped into  $M$  pairs:  $\{ \mathcal{T}^{(m,n)}, \text{perm}_{(2,1,3)}(\mathcal{T}^{(n,m)*}) \}$ , with fixed  $m$  and varying  $n$ . We concatenate each pair of tensors along the third mode into a new tensor that admits a PD, as:

$$\mathcal{T}^{(m,n)} \triangleq \begin{cases} \text{cat}(\mathcal{T}^{(m,n)}, \text{perm}_{(2,1,3)}(\mathcal{T}^{(n,m)*})) \\ = \left[ \mathbf{A}^{(m)}, \mathbf{A}^{(n)*}, [\mathbf{C}^{(m,n)}, \mathbf{C}^{(n,m)*}] \right]_R & m \leq n, \\ \text{cat}(\text{perm}_{(2,1,3)}(\mathcal{T}^{(n,m)*}), \mathcal{T}^{(m,n)}) \\ = \left[ \mathbf{A}^{(m)}, \mathbf{A}^{(n)*}, [\mathbf{C}^{(n,m)}, \mathbf{C}^{(m,n)*}] \right]_R & m > n. \end{cases} \quad (6)$$

The new set of tensors constructed by (6) admits a DC-CPD that has the conjugated symmetry:

$$\begin{cases} \mathcal{T}^{(m,n)} = \left[ \mathbf{A}^{(m)}, \mathbf{A}^{(n)*}, \mathbf{C}^{(m,n)} \right]_R, \\ \text{where } \mathcal{T}^{(m,n)} = \text{perm}_{(2,1,3)}(\mathcal{T}^{(n,m)*}). \end{cases} \quad (7)$$

The concatenated tensors  $\mathcal{T}^{(m,n)}$  have the advantage over  $\mathcal{T}^{(m,n)}$  that their third dimension is larger, which will make it easier to satisfy the full column rank assumption of the factor matrix in the third mode, as imposed by the derivation in the next section.

Because of the conjugated symmetry in DC-CPD, it suffices to consider the following set  $\Upsilon^{(m)}$  of tensors to take into account all occurrences of  $\mathbf{A}^{(m)}$ , for fixed  $m$ :

$$\Upsilon^{(m)} = \{ \mathcal{T}^{(m,n)} = \left[ \mathbf{A}^{(m)}, \mathbf{A}^{(n)*}, \mathbf{C}^{(m,n)} \right]_R, n = 1, \dots, M \}. \quad (8)$$

Note that in (8), seen as C-CPD, occurrences of  $\mathcal{A}^{(m)*}$  in the second mode are taken care of automatically because of the conjugated symmetry.

*Remark 2:* We note that DC-CPD (7) differs from existing C-CPD works in the following aspects: (i) DC-CPD (7) has a double coupling structure in the first two modes while C-CPD in [45]–[58] consider coupling in a single mode; (ii) the common factor matrix in DC-CPD (7) corresponds to the mixing matrix in J-BSS (2), and does not have full column rank if the J-BSS problem is underdetermined. The existing C-CPD works all assume that the common factor matrix has full column rank. In [59] it is assumed that at least one of the common factor matrices in a DC-CPD has full column rank. In what follows, we call a DC-CPD *overdetermined* if all the factor matrices  $\mathcal{A}^{(1)}, \dots, \mathcal{A}^{(M)}$  have full column rank. The DC-CPD is called *underdetermined* if it is not the case. Underdetermined DC-CPD may result from underdetermined J-BSS problems, in which one or more of the mixing matrices  $\mathcal{A}^{(1)}, \dots, \mathcal{A}^{(M)}$  have more columns than rows.

### III. ALGEBRAIC ALGORITHM

In this section, we introduce an algebraic algorithm for DC-CPD. We formally call an algorithm algebraic if it relies only on arithmetic operations, overdetermined sets of linear equations, matrix singular value decomposition (SVD) and generalized eigenvalue decomposition (GEVD). In particular, an algebraic computation does not involve a numerical optimization in which the cost function may have multiple local optima, or of which the convergence is not guaranteed.

#### A. Overall approach

If the DC-CPD (4) is *overdetermined*, we immediately have an algebraic solution. More precisely, any of the CPDs in (4) can be computed by GEVD [61]. This yields us the factor matrices  $\mathcal{A}^{(m)}$  and  $\mathcal{A}^{(n)}$  up to trivial scaling and permutation indeterminacies, for any choice of  $m$  and  $n$ . Assume for instance that  $\mathcal{A}^{(1)}$  has been found, then we can find all the remaining  $\mathcal{A}^{(n)}$ ,  $n = 2, \dots, M$ , from the CPD of  $\mathcal{T}^{(1,n)}$  for varying  $n$ . In fact, since in these CPDs the factor matrix  $\mathcal{A}^{(1)}$  is already known, the other factor matrices are obtained by mere rank-1 approximation of the matricized columns of [22]:

$$\mathbf{T}_1^{(1,n)} (\mathcal{A}^{(1)T})^\dagger = \mathcal{A}^{(n)*} \odot \mathcal{C}^{(1,n)}. \quad (9)$$

Indeed, each column of  $\mathcal{A}^{(n)*} \odot \mathcal{C}^{(1,n)}$  is a vectorized rank-1 matrix:

$$\text{unvec}(\mathbf{q}_{1,r}^{(1,n)}) = \mathbf{a}_r^{(n)*} \cdot \mathbf{c}_r^{(1,n)T}, \quad r=1, \dots, R, \quad (10)$$

where vector  $\mathbf{q}_{1,r}^{(1,n)}$  is the  $r$ th column of  $\mathbf{T}_1^{(1,n)} (\mathcal{A}^{(1)T})^\dagger$ . Continuing this way, all the factor matrices  $\mathcal{A}^{(m)}$  can be determined,  $m = 1, \dots, M$ . The overdetermined DC-CPD can also be computed by GJD algorithms proposed in [37]–[39], noting that GJD are essentially equivalent to DC-CPD in the overdetermined case.

If the DC-CPD (4) is *underdetermined*, it is still possible to derive an algebraic algorithm, which is the main concern of our work. The algebraic DC-CPD algorithm fits in the framework

of the algebraic algorithms in [10], [12], [13], [19], [20], [51], [52], which, by the use of a rank-1 or rank- $R$  detection mapping, convert a possibly underdetermined (coupled) CPD into an overdetermined CPD.

To make the derivation of our DC-CPD algorithm more accessible, we first give a high-level summary of the algebraic algorithm for underdetermined CPD in [10]. For more details, the reader is referred to [10].

First, the rank-1 detection mapping  $\Phi^{(R1)} : (\mathbf{X}, \mathbf{Y}) \in \mathbb{C}^{I \times J} \times \mathbb{C}^{I \times J} \rightarrow \Phi^{(R1)}(\mathbf{X}, \mathbf{Y}) \in \mathbb{C}^{I \times I \times J \times J}$  is defined as:

$$[\Phi^{(R1)}(\mathbf{X}, \mathbf{Y})]_{i,j,g,h} \triangleq x_{i,g} y_{j,h} + y_{i,g} x_{j,h} - x_{i,h} y_{j,g} - y_{i,h} x_{j,g}. \quad (11)$$

Three main properties of this rank-1 detection mapping are: (1) it is bilinear in its arguments:  $\Phi^{(R1)}(\sum_p \alpha_p \mathbf{X}_p, \sum_q \beta_q \mathbf{Y}_q) = \sum_p \sum_q \alpha_p \beta_q \Phi^{(R1)}(\mathbf{X}_p, \mathbf{Y}_q)$ ; (2) for a non-zero matrix  $\mathbf{X}$ ,  $\Phi^{(R1)}(\mathbf{X}, \mathbf{X})$  is a zero tensor if and only if  $\mathbf{X}$  is a rank-1 matrix; and (3) the rank-1 detection mapping is symmetric in its arguments  $\Phi^{(R1)}(\mathbf{X}, \mathbf{Y}) = \Phi^{(R1)}(\mathbf{Y}, \mathbf{X})$ .

To compute the CPD of a tensor  $\mathcal{T} = [\mathcal{A}, \mathcal{A}', \mathcal{C}]_R$ , where  $\mathcal{A} \in \mathbb{C}^{I \times R}$ ,  $\mathcal{A}' \in \mathbb{C}^{J \times R}$ , and  $\mathcal{C} \in \mathbb{C}^{R \times R}$ , the algebraic CPD algorithm in [10] now consists of the following main steps (note that only  $\mathcal{C}$  is required to have full column rank,  $\mathcal{A}$  and/or  $\mathcal{A}'$  can be rank-deficient, and we can allow  $I < R$  and/or  $J < R$ ):

(i) Apply the rank-1 detection mapping to the  $s$ th and  $u$ th frontal slices of  $\mathcal{T}$  to construct a tensor  $\Phi^{(R1)}(\mathcal{T}_{(\dots,s)}, \mathcal{T}_{(\dots,u)})$ , and reshape it into a vector of length  $I^2 J^2$ . We have  $R(R-1)/2$  such vectors for varying  $s$  and  $u$ ,  $1 \leq s < u \leq R$ . We stack these vectors into the columns of a  $I^2 J^2 \times R(R-1)/2$  matrix  $\Gamma$ .

(ii) We make the assumption that tensors  $\Phi^{(R1)}(\mathcal{T}_{(\dots,s)}, \mathcal{T}_{(\dots,u)})$  are linearly independent for  $1 \leq s < u \leq R$ . This assumption is very mild. It can be shown that generically it is satisfied as long as  $R(R-1) \leq IJ(I-1)(J-1)/2$ . Under this assumption we have:  $\dim(\ker(\Gamma)) = R$ , and the  $R$  basis vectors  $\mathbf{w}_1, \dots, \mathbf{w}_R$  in  $\ker(\Gamma)$  can be reshaped into a tensor that admits an overdetermined CPD  $\mathcal{W} = [\mathcal{B}, \mathcal{B}, \mathcal{F}]_R$ , where factor matrix  $\mathcal{B} = \tilde{\mathcal{C}}^{-T}$ , with  $\tilde{\mathcal{C}}$  equivalent to  $\mathcal{C}$  up to scaling and permutation ambiguities.

(iii) As the CPD  $\mathcal{W} = [\mathcal{B}, \mathcal{B}, \mathcal{F}]_R$  is overdetermined, it can be computed algebraically via GEVD, which makes use of two frontal slices of  $\mathcal{W}$ . We can also compute it via SD which makes use of all the frontal slices. Optimization based CPD algorithms such as alternating least squares (ALS), or nonlinear least squares (NLS) can be used to maximize the overall fit. Once  $\mathcal{B}$  has been computed, we immediately obtain  $\tilde{\mathcal{C}} = \mathcal{B}^{-T}$ , and the remaining factor matrices  $\mathcal{A}$  and  $\mathcal{A}'$  can be recovered using the CPD structure of the data tensor.

For DC-CPD, first recall that the factor matrices can be directly computed via GEVD, if it is overdetermined. If the original DC-CPD is underdetermined, we start from the formulation (8), and derive the algebraic algorithm following a similar line of thought as for its CPD counterpart. The derivation consists of the following main steps:

(i) We will propose a variant of rank-1 detection mapping (11), namely a coupled rank-1 detection mapping (12), and a corresponding vector operator  $\psi(\cdot)$  (13). We perform  $\psi(\cdot)$  on all the combinations of  $K$  tensors  $\mathcal{T}^{(m,n_1)}, \dots, \mathcal{T}^{(m,n_K)}$  in  $\Upsilon^{(m)}$ ,

which share a common factor matrix  $\mathbf{A}^{(m)}$  to obtain matrices  $\mathbf{\Gamma}^{(m, n_1, \dots, n_K)}$ ,  $m = 1, \dots, M$ ,  $1 \leq n_1 < \dots < n_K \leq M$ ,  $K = 2, \dots, M$ .

(ii) We assume that the vectors  $\boldsymbol{\psi}(\mathbf{a}_{r_1}^{(m)} \mathbf{a}_{r_1}^{(n_1)H}, \dots, \mathbf{a}_{r_K}^{(m)} \mathbf{a}_{r_K}^{(n_K)H})$ , where each  $(r_1, \dots, r_K)$  contains at least two distinct indices, are linearly independent. This assumption is more relaxed than its CPD counterpart, as will be shown later. Under this assumption, we have  $\dim(\ker(\mathbf{\Gamma}^{(m, n_1, \dots, n_K)})) = R$ , and the  $R$  basis vectors  $\mathbf{w}_1^{(m, n_1, \dots, n_K)}, \dots, \mathbf{w}_R^{(m, n_1, \dots, n_K)}$  in  $\ker(\mathbf{\Gamma}^{(m, n_1, \dots, n_K)})$  can be reshaped into a  $(K+1)$ th-order tensor  $\mathcal{W}^{(m, n_1, \dots, n_K)}$ . This tensor admits an overdetermined CPD, involving  $\mathbf{B}^{(m, n_1)}, \dots, \mathbf{B}^{(m, n_K)}$  as factor matrices, where  $\mathbf{B}^{(m, n_k)} = \tilde{\mathbf{C}}^{(m, n_k)-T}$ , with  $\tilde{\mathbf{C}}^{(m, n_k)}$  equivalent to  $\mathbf{C}^{(m, n_k)}$  up to scaling and permutation ambiguities. For varying indices  $m, n_1, \dots, n_K$ , the above steps generate a set of tensors. These tensors together admit an overdetermined C-CPD with coupling in multiple modes.

(iii) We will compute the overdetermined C-CPD to obtain the factor matrices  $\mathbf{B}^{(m, n)}$ ,  $m, n = 1, \dots, M$ . This can be done algebraically by means of a GEVD, using two tensor slices. It can also be computed via matrix simultaneous diagonalization (SD) based scheme, using all tensor slices. Optimization based algorithms, such as those based on ALS and structured data fusion (SDF, [63]) can be used to maximize the overall fit. The matrix  $\mathbf{C}^{(m, n)}$  can be calculated as the inverse of  $\mathbf{B}^{(m, n)}$  up to trivial indeterminacies. Once  $\mathbf{C}^{(m, n)}$  is known, the remaining factor matrices  $\mathbf{A}^{(m)}$  can be recovered using the DC-CPD structure of the data tensors.

### B. Basic assumptions

We assume both  $\mathbf{A}^{(m)} \odot \mathbf{A}^{(n)*}$  and  $\mathbf{C}^{(m, n)}$  have full column rank, for all the indices  $m, n$ . Together these assumptions imply that the rank of tensor  $\mathcal{T}^{(m, n)}$  is equal to the rank of the mode-3 matrix representation  $\mathbf{T}_3^{(m, n)}$ . This is of practical use in the sense that the number of sources can be determined by checking the number of significant singular values of  $\mathbf{T}_3^{(m, n)}$ . We note that DC-CPD (8) is not unique if  $\mathbf{A}^{(m)} \odot \mathbf{A}^{(n)*}$  does not have full column rank. In fact, in this case a decomposition in a smaller number of terms is possible. For instance, if  $\mathbf{a}_R^{(m)} \otimes \mathbf{a}_R^{(n)*} = \sum_{r=1}^{R-1} \mathbf{a}_r^{(m, n)} \mathbf{a}_r^{(m)} \otimes \mathbf{a}_r^{(n)*}$ , then  $\mathcal{T}^{(m, n)} = \sum_{r=1}^{R-1} \mathbf{a}_r^{(m)} \otimes \mathbf{a}_r^{(n)*} \otimes (\mathbf{c}_r^{(m, n)} + \mathbf{a}_r^{(m, n)} \mathbf{c}_R^{(m, n)})$ . On the other hand, if  $\mathbf{C}^{(m, n)}$  does not have full column rank, decomposition (4) may still be unique (for instance, algebraic algorithms for CPD have been derived for cases where none of the factor matrices has full column rank [12], [13]), while the rank of tensor  $\mathcal{T}^{(m, n)}$  is not equal to the rank of the mode-3 matrix representation  $\mathbf{T}_3^{(m, n)}$ . Here we do not consider this more complicated case. In addition, we make the notational assumption that the factor matrices  $\mathbf{C}^{(m, n)}$  in the third mode have size  $R \times R$ . In practice, this can always be achieved by a classical dimensionality reduction step: if the columns of a matrix  $\mathbf{U}^{(m, n)}$  form an orthonormal basis of the row space of  $\mathbf{T}_3^{(m, n)}$ , then  $\mathbf{T}_3^{(m, n)} \mathbf{U}^{(m, n)}$  has  $R$  columns, tensor  $\text{Ten}(\mathbf{T}_3^{(m, n)} \mathbf{U}^{(m, n)}, I, I, R)$  has reduced dimensionality  $R$  in the third mode, and its factor matrices are  $\mathbf{A}^{(m)}$ ,  $\mathbf{A}^{(n)*}$ , and  $\mathbf{U}^{(m, n)T} \mathbf{C}^{(m, n)} \in \mathbb{C}^{R \times R}$ .

### C. Coupled rank-1 detection

We give the following two definitions and a theorem.

*Definition 1:* Matrices  $\mathbf{X}^{(1)} \in \mathbb{C}^{N \times J_1}, \dots, \mathbf{X}^{(K)} \in \mathbb{C}^{N \times J_K}$  are said to be coupled rank-1 matrices if they are all rank-1 and have the same column space.

*Definition 2:* The coupled rank-1 detection mapping  $\Phi_{(v, w)}$ :  $(\mathbf{X}^{(1)}, \dots, \mathbf{X}^{(K)}) \in \mathbb{C}^{N \times J_1} \times \dots \times \mathbb{C}^{N \times J_K} \rightarrow \Phi_{(v, w)}(\mathbf{X}^{(1)}, \dots, \mathbf{X}^{(K)}) \in \mathbb{C}^{N \times \dots \times N \times J_1 \times \dots \times J_K}$  is defined by:

$$\left[ \Phi_{(v, w)}(\mathbf{X}^{(1)}, \dots, \mathbf{X}^{(K)}) \right]_{i_1 \dots i_K, j_1 \dots j_K} \triangleq \begin{bmatrix} \mathbf{x}_{i_v, j_v}^{(v)} & \mathbf{x}_{i_w, j_w}^{(w)} \\ \mathbf{x}_{i_w, j_w}^{(v)} & \mathbf{x}_{i_v, j_v}^{(w)} \end{bmatrix} \prod_{l \notin \{v, w\}} \mathbf{x}_{i_l, j_l}^{(l)}, \quad (12)$$

with  $1 \leq v < w \leq K$ . The number of arguments of  $\Phi_{(v, w)}$ ,  $K$ , is called the order, and the subscript  $(v, w)$  is called the index of the coupled rank-1 detection mapping, respectively.

*Theorem 1:* For  $K$  nonzero matrices  $\mathbf{X}^{(k)} \in \mathbb{C}^{N \times J_k}$ ,  $k = 1, \dots, K$ , consider the vector  $\boldsymbol{\psi}(\mathbf{X}^{(1)}, \dots, \mathbf{X}^{(K)})$  of length  $\mathbf{C}_K^2 N^K \prod_{k=1}^K J_k$  obtained via the coupled rank-1 detection mapping (12):

$$\boldsymbol{\psi}(\mathbf{X}^{(1)}, \dots, \mathbf{X}^{(K)}) \triangleq \begin{bmatrix} \text{vec}(\Phi_{(1,2)}(\mathbf{X}^{(1)}, \dots, \mathbf{X}^{(K)})) \\ \text{vec}(\Phi_{(1,3)}(\mathbf{X}^{(1)}, \dots, \mathbf{X}^{(K)})) \\ \vdots \\ \text{vec}(\Phi_{(K-1, K)}(\mathbf{X}^{(1)}, \dots, \mathbf{X}^{(K)})) \end{bmatrix}. \quad (13)$$

Then  $\boldsymbol{\psi}(\mathbf{X}^{(1)}, \dots, \mathbf{X}^{(K)})$  is a zero vector if and only if its arguments  $\mathbf{X}^{(1)}, \dots, \mathbf{X}^{(K)}$  are coupled rank-1 matrices.

The proof of *Theorem 1* is given in the *Appendix*. We note that the above definitions and theorem generalize the rank-1 detection mapping and relevant results [10], [12], [13], [19], [20], [51], [52] to the coupled case.

Next we explain how to use the coupled rank-1 detection mapping to transform an underdetermined DC-CPD into an overdetermined C-CPD. For clarity, we first explain the simplest case where  $K = 2$ , and then address the general case where  $K \geq 2$ .

### D. The simplest case: $K = 2$

We first formulate a theorem that provides deterministic conditions for which DC-CPD is unique and for which DC-CPD can be calculated algebraically.

*Theorem 2:* Let  $\mathcal{T}^{(m, l)} = \llbracket \mathbf{A}^{(m)}, \mathbf{A}^{(l)*}, \mathbf{C}^{(m, l)} \rrbracket_R$ , where  $l \in \{p, q\}$ . Assume that  $\mathbf{C}^{(m, p)}, \mathbf{C}^{(m, q)}$  have full column rank for all  $1 \leq p < q \leq M$ ,  $m = 1, \dots, M$ , and that  $\boldsymbol{\psi}(\mathbf{a}_r^{(m)} \mathbf{a}_r^{(p)H}, \mathbf{a}_r^{(m)} \mathbf{a}_r^{(q)H}) = (\mathbf{a}_r^{(m)} \otimes \mathbf{a}_r^{(m)} - \mathbf{a}_r^{(m)} \otimes \mathbf{a}_r^{(m)}) \otimes \mathbf{a}_r^{(p)*} \otimes \mathbf{a}_r^{(q)*}$  are linearly independent for  $1 \leq t \neq r \leq R$ . Then we have:

- Tensors  $\mathcal{T}^{(m, n)}$ , for all  $m, n = 1, \dots, M$ , admit a DC-CPD, i.e. they consist of the sum of  $R$  double coupled rank-1 terms, and the number of terms cannot be reduced.
- The DC-CPD is unique.
- The DC-CPD can be calculated algebraically.

Next we derive the algebraic DC-CPD algorithm. Note that the derivation provides a constructive proof of *Theorem 2*. The main idea is to transform the original underdetermined DC-CPD into an overdetermined DC-CPD through the use of the coupled rank-1 detection mapping. All the factor matrices involved in this overdetermined DC-CPD have full column rank, and thus can be calculated algebraically via GEVD. If the



original DC-CPD is already overdetermined, then the rank-1 detection mapping need not be used, and the factor matrices can be directly computed via GEVD or SD.

(i) Construct matrix  $\mathbf{F}^{(m,p,q)}$  via coupled rank-1 detection.

When  $K = 2$ , the coupled rank-1 detection mapping defined in (12) simplifies to:

$$\left[ \Phi_{(1,2)}(\mathbf{X}^{(1)}, \mathbf{X}^{(2)}) \right]_{i,j,g,h} \triangleq \begin{bmatrix} x_{i,g}^{(1)} & x_{i,h}^{(2)} \\ x_{j,g}^{(1)} & x_{j,h}^{(2)} \end{bmatrix} = x_{i,g}^{(1)} x_{j,h}^{(2)} - x_{j,g}^{(1)} x_{i,h}^{(2)}. \quad (14)$$

The vector  $\psi(\mathbf{X}^{(1)}, \mathbf{X}^{(2)})$  defined in (13) is now equal to  $\text{vec}(\Phi_{(1,2)}(\mathbf{X}^{(1)}, \mathbf{X}^{(2)}))$ . From *Theorem 1* we know that  $\Phi_{(1,2)}(\mathbf{X}^{(1)}, \mathbf{X}^{(2)})$  is a zero tensor if and only if  $\mathbf{X}^{(1)}, \mathbf{X}^{(2)}$  are coupled rank-1 matrices.

For each pair of tensors  $\mathcal{T}^{(m,p)}, \mathcal{T}^{(m,q)} \in \Upsilon^{(m)}$ , we use the operation  $\Phi_{(1,2)}(\cdot)$  on the  $s$ th frontal slice of the former, and the  $u$ th frontal slice of the latter,  $1 \leq s, u \leq R$ :

$$\left[ \Phi_{(1,2)}(\mathcal{T}_{(:, :, s)}^{(m,p)}, \mathcal{T}_{(:, :, u)}^{(m,q)}) \right]_{i,j,g,h} = t_{i,g,s}^{(m,p)} t_{j,h,u}^{(m,q)} - t_{j,g,s}^{(m,p)} t_{i,h,u}^{(m,q)}. \quad (15)$$

We vectorize  $\Phi_{(1,2)}(\mathcal{T}_{(:, :, s)}^{(m,p)}, \mathcal{T}_{(:, :, u)}^{(m,q)})$  into vectors  $\psi(\mathcal{T}_{(:, :, s)}^{(m,p)}, \mathcal{T}_{(:, :, u)}^{(m,q)})$ , and stack these vectors into the columns of a  $N^4 \times R^2$  matrix  $\mathbf{F}^{(m,p,q)}$ . Note that  $\mathbf{F}^{(m,p,q)}$  is a DC-CPD variant of the matrix  $\mathbf{F}$  for CPD in step (i) of *Subsection III.A*.

(ii) Construct tensor  $\mathcal{W}^{(m,p,q)}$  in  $\ker(\mathbf{F}^{(m,p,q)})$ . For varying  $m, p, q$ , these tensors admit an overdetermined DC-CPD.

For fixed  $m, p, q$ , recall that by assumption  $\psi(\mathbf{a}_t^{(m)} \mathbf{a}_t^{(p)H}, \mathbf{a}_r^{(m)} \mathbf{a}_r^{(q)H})$  are linearly independent,  $t \neq r$ . With a short derivation analogous to equation (2.9)–(2.13) in [10], we obtain the result that there exist precisely  $R$  linearly independent matrices  $\mathbf{V}_l^{(m,p,q)} \in \mathbb{C}^{R \times R}$ ,  $l = 1, \dots, R$ , such that:

$$\sum_{s,u=1}^R (\mathbf{V}_l^{(m,p,q)})_{s,u} \psi(\mathcal{T}_{(:, :, s)}^{(m,p)}, \mathcal{T}_{(:, :, u)}^{(m,q)}) = \mathbf{0}. \quad (16)$$

Moreover, the matrices  $\mathbf{B}^{(m,p)}, \mathbf{B}^{(m,q)}$  simultaneously diagonalize  $\mathbf{V}_l^{(m,p,q)}$ :

$$\mathbf{V}_l^{(m,p,q)} = \mathbf{B}^{(m,p)} \cdot \mathbf{A}_l^{(m,p,q)} \cdot \mathbf{B}^{(m,q)T}, \quad (17)$$

where  $\mathbf{A}_l^{(m,p,q)}$  is a diagonal matrix,  $\mathbf{B}^{(m,p)} = \tilde{\mathbf{C}}^{(m,p)-T} \in \mathbb{C}^{R \times R}$ ,  $\mathbf{B}^{(m,q)} = \tilde{\mathbf{C}}^{(m,q)-T} \in \mathbb{C}^{R \times R}$ ,  $\tilde{\mathbf{C}}^{(m,p)} \triangleq (\mathbf{C}^{(m,p)} \mathbf{D}_C^{(m,p)} \mathbf{\Pi})$ ,  $(\mathbf{C}^{(m,q)} \mathbf{D}_C^{(m,q)} \mathbf{\Pi})$ ,  $\mathbf{D}_C^{(m,p)}, \mathbf{D}_C^{(m,q)}$  are diagonal matrices, and  $\mathbf{\Pi}$  is a common permutation matrix for  $\mathbf{B}^{(m,p)}, \mathbf{B}^{(m,q)}$ .

Equation (16) shows that  $\mathbf{V}_l^{(m,p,q)}$  is the reshaped version of vector  $\mathbf{w}_l^{(m,p,q)} \in \ker(\mathbf{F}^{(m,p,q)})$ . Note that the number of linearly independent  $\mathbf{V}_l^{(m,p,q)}$  is precisely  $R$ . As such, we can compute a set of  $R$  basis vectors in  $\ker(\mathbf{F}^{(m,p,q)})$  to obtain the matrices  $\mathbf{V}_l^{(m,p,q)}$ . In addition, (17) shows that we can stack the matrices  $\mathbf{V}_l^{(m,p,q)}$  along the third mode into a tensor:  $(\mathcal{W}^{(m,p,q)})_{:, :, l} \triangleq \mathbf{V}_l^{(m,p,q)}$ , which admits a third-order CPD, for fixed  $m, p, q$ :

$$\mathcal{W}^{(m,p,q)} = \left[ \mathbf{B}^{(m,p)}, \mathbf{B}^{(m,q)}, \mathbf{F}^{(m,p,q)} \right]_R, \quad (18)$$

where  $\mathbf{F}^{(m,p,q)} \in \mathbb{C}^{R \times R}$  holds the diagonal entries of  $\mathbf{A}_l^{(m,p,q)}$  as its  $l$ th row. Recall that  $\mathbf{C}^{(m,p)}, \mathbf{C}^{(m,q)}$  have full column rank by assumption, and thus  $\mathbf{B}^{(m,p)}, \mathbf{B}^{(m,q)}$  also have full column rank. In addition,  $\mathbf{V}_l^{(m,p,q)}$  for fixed  $(m, p, q)$  and varying  $l$  are linearly independent, as they correspond to a set of basis vectors of

$\ker(\mathbf{F}^{(m,p,q)})$ . According to (17), the diagonal matrices  $\mathbf{A}_l^{(m,p,q)}$  are linearly independent as well. Therefore,  $\mathbf{F}^{(m,p,q)}$  also has full rank. As such, all the three factor matrices of  $\mathcal{W}^{(m,p,q)}$  have full column rank, and  $\mathcal{W}^{(m,p,q)}$  admits a CPD that is overdetermined.

In (15)–(18), we have used the coupled rank-1 detection mapping (14) to convert the decomposition of a pair of coupled tensors into an unsymmetric overdetermined third-order CPD. For the overall DC-CPD (8), we perform the same procedure for all pairs of coupled tensors and obtain a set of overdetermined CPDs. With varying indices  $(m, p, q)$ ,  $m = 1, \dots, M$ ,  $1 \leq p < q \leq M$ , the CPDs (18) together form an overdetermined third-order DC-CPD with coupling in the first two modes. Note that the derivation in this subsection is in analogy with that in CPD step (ii) in *Subsection III.A*.

(iii) Solve the overdetermined DC-CPD (18), and calculate factor matrices  $\mathbf{A}^{(1)}, \dots, \mathbf{A}^{(M)}$ .

As the new DC-CPD (18) is overdetermined, it admits an algebraic solution. There are different ways to compute this solution. First, as all the factor matrices have full column rank, any of the CPDs (18) can be computed by GEVD [61]. This yields us the factor matrices  $\mathbf{B}^{(m,p)}$  and  $\mathbf{B}^{(m,q)}$  up to trivial scaling and permutation indeterminacies, for any choice of  $m, p$  and  $q$ . Assume for instance that  $\mathbf{B}^{(m,1)}$  has been found, then we can find all remaining  $\mathbf{B}^{(m,q)}$  and  $\mathbf{F}^{(m,1,q)}$  from the CPD of  $\mathcal{W}^{(m,1,q)}$  for fixed  $m$  and varying  $q$ . In fact, since in these CPDs the factor matrix  $\mathbf{B}^{(m,1)}$  is already known, the other factor matrices follow from rank-1 approximation of the matrixized columns of [22]:

$$\mathbf{W}_1^{(m,1,q)} \mathbf{B}^{(m,1)-T} = \mathbf{B}^{(m,q)} \odot \mathbf{F}^{(m,1,q)}. \quad (19)$$

Indeed, each column of  $\mathbf{B}^{(m,q)} \odot \mathbf{F}^{(m,1,q)}$  is a vectorized rank-1 matrix:

$$\text{unvec}(\mathbf{q}_{1,r}^{(m,1,q)}) = \mathbf{b}_r^{(m,q)} \cdot \mathbf{f}_r^{(m,1,q)T}, \quad r=1, \dots, R, \quad (20)$$

where vector  $\mathbf{q}_{1,r}^{(m,1,q)}$  of length  $R^2$  is the  $r$ th column of  $\mathbf{W}_1^{(m,1,q)} \mathbf{B}^{(m,1)-T}$ . Continuing this way, all factor matrices  $\mathbf{B}^{(m,n)}$  can be determined,  $m, n = 1, \dots, M$ .

Besides the above mentioned GEVD based scheme, which makes use of two frontal slices of the data tensor, we may consider computing any of the CPDs (18) via SD, and then follow a similar strategy as the one above, to solve the DC-CPD. We may also consider computing the DC-CPD of all the tensors  $\mathcal{W}^{(m,p,q)}$  in (18) simultaneously via an optimization based algorithm, while taking the coupling structure into account. Several options are: (a) the framework of SDF is well-suited for the task; (b) ALS is a specific type of optimization algorithm that can be used. The updating equations can be explicitly derived in analogy with the derivation in the *Supplementary materials* for DC-CPD. Note that the GEVD based approach can be used to efficiently initialize these optimization based algorithms.

Now that the overdetermined DC-CPD has been computed, we obtain  $\tilde{\mathbf{C}}^{(m,n)} = \mathbf{C}^{(m,n)} \mathbf{D}_C^{(m,n)} \mathbf{\Pi} = \mathbf{B}^{(m,n)-T}$ , and  $\tilde{\mathbf{A}}^{(m)} \odot \tilde{\mathbf{A}}^{(n)*} = \mathbf{T}_3^{(m,n)} \mathbf{B}^{(m,n)}$ , where  $\tilde{\mathbf{A}}^{(m)} = \mathbf{A}^{(m)} \mathbf{D}_A^{(m)} \mathbf{\Pi}$  and  $\tilde{\mathbf{A}}^{(n)} = \mathbf{A}^{(n)} \mathbf{D}_A^{(n)} \mathbf{\Pi}$

are estimates of  $\mathbf{A}^{(m)}$  and  $\mathbf{A}^{(n)}$  up to scaling and permutation ambiguities,  $m, n = 1, \dots, M$ . Matrices  $\mathbf{D}_A^{(m)}$  and  $\mathbf{D}_A^{(n)}$  are diagonal matrices, and  $\mathbf{D}_A^{(m)} \mathbf{D}_A^{(n)*} \mathbf{D}_C^{(m,n)} = \mathbf{I}_R$ . We define  $\mathbf{G}_r^{(m,n)} \triangleq \text{unvec}(\mathbf{T}_3^{(m,n)} \mathbf{B}^{(m,n)})_{(:,r)}$ , and collect these matrices in a  $NM \times NM$  matrix  $\mathbf{G}_r$  as follows:

$$\mathbf{G}_r = \begin{bmatrix} \mathbf{G}_r^{(1,1)} & \dots & \mathbf{G}_r^{(1,M)} \\ \vdots & \ddots & \vdots \\ \mathbf{G}_r^{(M,1)} & \dots & \mathbf{G}_r^{(M,M)} \end{bmatrix} = \begin{bmatrix} \tilde{\mathbf{a}}_r^{(1)} \\ \vdots \\ \tilde{\mathbf{a}}_r^{(M)} \end{bmatrix} \cdot [\tilde{\mathbf{a}}_r^{(1)H}, \dots, \tilde{\mathbf{a}}_r^{(M)H}], \quad (21)$$

where  $\tilde{\mathbf{a}}_r^{(m)}$  denotes the  $r$ th column of  $\tilde{\mathbf{A}}^{(m)}$ ,  $r = 1, \dots, R$ ,  $m = 1, \dots, M$ . We can calculate  $[\tilde{\mathbf{a}}_r^{(1)T}, \dots, \tilde{\mathbf{a}}_r^{(M)T}]^T$  as the dominant eigenvector of  $\mathbf{G}_r$ .

We summarize the algebraic algorithm for  $K = 2$  in Table I.

TABLE I  
DC-CPD: ALGEBRAIC ALGORITHM FOR  $K = 2$

<b>Input:</b> $\{\mathcal{T}^{(m,n)} \in \mathbb{C}^{N \times N \times R} \mid 1 \leq m, n \leq M\}$ admitting DC-CPD (7).
1: Group $\mathcal{T}^{(m,n)}$ into $M$ sets $\Upsilon^{(m)}$ by (8).
2: For each pair of tensors $\mathcal{T}^{(m,p)}, \mathcal{T}^{(m,q)} \in \Upsilon^{(m)}$ , perform second-order coupled rank-1 detection mapping (15), for all frontal slices $\mathbf{T}_{(:,s)}^{(m,p)}, \mathbf{T}_{(:,s)}^{(m,q)}$ , to obtain tensors $\Phi_{(1,2)}(\mathbf{T}_{(:,s)}^{(m,p)}, \mathbf{T}_{(:,s)}^{(m,q)})$ , $1 \leq s, u \leq R$ . Vectorize these tensors and stack them into the columns of matrix $\mathbf{I}^{(m,p,q)}$ .
3: Calculate a set of $R$ basis vectors $\mathbf{w}_l^{(m,p,q)}$ in $\ker(\mathbf{I}^{(m,p,q)})$ , and reshape these vectors into matrices $\mathbf{V}_l^{(m,p,q)}$ , $l = 1, \dots, R$ . Stack $\mathbf{V}_l^{(m,p,q)}$ with varying $l$ into a tensor $\mathcal{W}^{(m,p,q)}$ . For varying $m, p, q$ , the tensors $\mathcal{W}^{(m,p,q)}$ together admit an overdetermined DC-CPD (18).
4: Solve (18) to compute the matrices $\mathbf{B}^{(m,n)}$ . Then we have $\tilde{\mathbf{C}}^{(m,n)} = \mathbf{B}^{(m,n)-T}$ and $\tilde{\mathbf{A}}^{(m)} \odot \tilde{\mathbf{A}}^{(n)*} = \mathbf{T}_3^{(m,n)} \mathbf{B}^{(m,n)}$ .
5: Compute matrix $\mathbf{G}_r$ by (21). Then the $r$ th column of the factor matrices $\tilde{\mathbf{A}}^{(m)}$ can be computed as the dominant eigenvector of $\mathbf{G}_r$ , $m = 1, \dots, M$ , $r = 1, \dots, R$ .
<b>Output:</b> Estimates of the factor matrices $\tilde{\mathbf{A}}^{(m)}$ and $\tilde{\mathbf{C}}^{(m,n)}$ , $1 \leq m, n \leq M$ .

### E. The general case: $K \in [2, M]$

Let us now generalize our results to arbitrary  $K \in [2, M]$ , denoting the order of the coupled rank-1 detection mapping. A larger  $K$  generally relaxes the uniqueness condition, but also increases the computational complexity, as will be explained later. In practice one may start with  $K = 2$ , and increase its value if the number of sources that can be handled is not sufficient.

For a chosen constant  $K \in [2, M]$ , we first formulate a theorem that provides deterministic conditions for which DC-CPD is unique, and for which DC-CPD can be calculated algebraically. Note that this theorem extends *Theorem 2* for  $K = 2$  to  $K \in [2, M]$ .

*Theorem 3:* Let  $\mathcal{T}^{(m,n_k)} = \llbracket \mathbf{A}^{(m)}, \mathbf{A}^{(n_k)*}, \mathbf{C}^{(m,n_k)} \rrbracket_R \in \Upsilon^{(m)}$ , where  $m, n_k = 1, \dots, M$ ,  $k = 1, \dots, K$ , and  $K \in [2, M]$  is a preset constant. We assume, for all values  $1 \leq n_1 < \dots < n_K \leq M$  and  $m = 1, \dots, M$ , that matrices  $\mathbf{C}^{(m,n_k)}$  and  $\Phi_{n_1, \dots, n_K}^{(m)}$  have full column rank. Here  $\Phi_{n_1, \dots, n_K}^{(m)}$  holds vectors  $\psi(\mathbf{a}_{n_1}^{(m)} \mathbf{a}_{n_1}^{(n_k)H}, \dots, \mathbf{a}_{n_K}^{(m)} \mathbf{a}_{n_K}^{(n_k)H})$  as its columns. These columns are indexed by  $(r_1, \dots, r_K) \in \Theta^{(K)}$ , where  $\Theta^{(K)}$  is a set of tuples  $(r_1, \dots, r_K)$ ,  $1 \leq r_1 \leq \dots \leq r_K \leq R$ , in which each tuple contains at least two distinct elements. Then we have:

- Tensors  $\mathcal{T}^{(m,n)}$ , for varying  $m, n = 1, \dots, M$ , admit a DC-CPD, i.e. they consist of the sum of  $R$  double coupled rank-1 terms, and the number of terms cannot be reduced.

- The DC-CPD is unique.
- The DC-CPD can be calculated algebraically.

Next, we derive the algebraic DC-CPD algorithm for  $K \in [2, M]$ . This derivation is in analogy with the derivation for  $K = 2$ . It provides a constructive proof of *Theorem 3*.

(i) *Construct matrix  $\mathbf{I}^{(m,n_1, \dots, n_K)}$  via coupled rank-1 detection.*

We select  $K$  tensors  $\mathcal{T}^{(m,n_1)}, \dots, \mathcal{T}^{(m,n_K)}$  from  $\Upsilon^{(m)}$  (8),  $1 \leq n_1 < \dots < n_K \leq M$ . There are  $\mathbf{C}_M^K$  such  $K$ -combinations. For each  $K$ -combination  $\mathcal{T}^{(m,n_1)}, \dots, \mathcal{T}^{(m,n_K)} \in \Upsilon^{(m)}$ , we perform the operation (13) on all the possible combinations of the frontal slices of  $\mathcal{T}^{(m,n_1)}, \dots, \mathcal{T}^{(m,n_K)}$  to obtain a  $(K+1)$ th-order tensor  $\mathcal{G}^{(m,n_1, \dots, n_K)}$  of size  $(\mathbf{C}_K^2 N^{2K}) \times R \times \dots \times R$ :

$$[\mathcal{G}^{(m,n_1, \dots, n_K)}]_{(:,r_1, \dots, r_K)} \triangleq \psi(\mathbf{T}_{(:,r_1)}^{(m,n_1)}, \dots, \mathbf{T}_{(:,r_K)}^{(m,n_K)}), \quad (22)$$

where  $1 \leq r_k \leq R$ ,  $1 \leq k \leq K$ . Note that operation (22) implicitly uses the  $K$ th-order coupled rank-1 detection mapping (12). We reshape  $\mathcal{G}^{(m,n_1, \dots, n_K)}$  into a  $(\mathbf{C}_K^2 N^{2K}) \times R^K$  matrix  $\mathbf{I}^{(m,n_1, \dots, n_K)}$  as:

$$[\mathbf{I}^{(m,n_1, \dots, n_K)}]_{(l,:)} \triangleq \text{vec}([\mathcal{G}^{(m,n_1, \dots, n_K)}]_{(l,:)}), \quad (23)$$

where  $1 \leq l \leq \mathbf{C}_K^2 N^{2K}$ . Due to the multilinearity of  $\psi$ , and by making use of the property that  $\psi(\mathbf{a}_{n_1}^{(m)} \mathbf{a}_{n_1}^{(n_1)H}, \dots, \mathbf{a}_{n_K}^{(m)} \mathbf{a}_{n_K}^{(n_K)H}) = \mathbf{0}$  when  $r_1 = \dots = r_K$  (*Theorem 1*), we have the following result after a short derivation given in the *Supplementary materials*:

$$\mathbf{I}^{(m,n_1, \dots, n_K)} = \Phi_{n_1, \dots, n_K}^{(m)} \left( \mathbf{P}_{n_1, \dots, n_K}^{(m)} \right)^T, \quad (24)$$

where the  $(\mathbf{C}_K^2 N^{2K}) \times (R^K - R)$  matrix  $\Phi_{n_1, \dots, n_K}^{(m)}$  is defined in *Theorem 3*. The  $R^K \times (R^K - R)$  matrix  $\mathbf{P}_{n_1, \dots, n_K}^{(m)}$  has  $\mathbf{e}_{r_1}^{(m,n_1)} \otimes \dots \otimes \mathbf{e}_{r_K}^{(m,n_K)}$  as its columns. These columns are indexed by tuples  $(r_1, \dots, r_K) \in \Theta^{(K)}$ , where  $\Theta^{(K)}$  is defined in *Theorem 3*. We note that  $\mathbf{I}^{(m,n_1, \dots, n_K)}$  is the generalization of matrix  $\mathbf{I}^{(m,p,q)}$  in step (i) of *Subsection III.D* from  $K = 2$  to  $K \in [2, M]$ .

(ii) *Construct tensor  $\mathcal{W}^{(m,n_1, \dots, n_K)}$  in  $\ker(\mathbf{I}^{(m,n_1, \dots, n_K)})$ . For varying  $(m, n_1, \dots, n_K)$ , these tensors admit a  $(K+1)$ th-order overdetermined C-CPD with coupling in the first  $K$  modes.*

We give a theorem implying that the basis vectors in the null space of  $\mathbf{I}^{(m,n_1, \dots, n_K)}$  can be reshaped into a tensor that admits an overdetermined  $(K+1)$ th-order CPD.

*Theorem 4:* Let  $\mathcal{T}^{(m,n_k)} = \llbracket \mathbf{A}^{(m)}, \mathbf{A}^{(n_k)*}, \mathbf{C}^{(m,n_k)} \rrbracket_R \in \Upsilon^{(m)}$ ,  $k = 1, \dots, K$ ,  $1 \leq n_1 < \dots < n_K \leq M$ , and assume that  $\Phi_{n_1, \dots, n_K}^{(m)}$  in (24) and  $\mathbf{C}^{(m,n_k)}$  for all values of  $k$  have full column rank for fixed  $(m, n_1, \dots, n_K)$ , then we have:

- $\ker(\mathbf{I}^{(m,n_1, \dots, n_K)}) = \ker((\mathbf{P}_{n_1, \dots, n_K}^{(m)})^T)$ .
- $\dim(\ker(\mathbf{I}^{(m,n_1, \dots, n_K)})) = R$ .
- The basis vectors  $\mathbf{w}_r^{(m,n_1, \dots, n_K)}$  in  $\ker(\mathbf{I}^{(m,n_1, \dots, n_K)})$ ,  $r = 1, \dots, R$ , can be written as linear combinations of the vectors  $\mathbf{b}_u^{(m,n_1)} \otimes \dots \otimes \mathbf{b}_u^{(m,n_K)}$ ,  $u = 1, \dots, R$ :

$$\mathbf{w}_r^{(m,n_1, \dots, n_K)} = \sum_{u=1}^R \mathbf{f}_{r,u}^{(m,n_1, \dots, n_K)} \cdot \mathbf{b}_u^{(m,n_1)} \otimes \dots \otimes \mathbf{b}_u^{(m,n_K)} \in \mathbb{C}^{R^K}, \quad (25)$$

where  $[\mathbf{b}_1^{(m,n_1)}, \dots, \mathbf{b}_R^{(m,n_1)}] = \mathbf{B}^{(m,n_1)} = \tilde{\mathbf{C}}^{(m,n_1)-T} \in \mathbb{C}^{R \times R}$ ,  $\tilde{\mathbf{C}}^{(m,n_k)} \triangleq (\mathbf{C}^{(m,n_k)} \mathbf{D}_C^{(m,n)} \mathbf{\Pi})$ ,  $\mathbf{D}_C^{(m,n)}$  is a diagonal matrix, and  $\mathbf{\Pi}$  is a common permutation matrix for all  $\mathbf{B}^{(m,n_k)}$ ,  $k = 1, \dots, K$ .

We give the proof of this theorem in the *Appendix*. This theorem provides the following key results for the algebraic

algorithm: (a) the dimension of the null space of  $\mathbf{F}^{(m,n_1,\dots,n_K)}$  reveals the number of sources; (b) via (25), the basis vectors in the null space of  $\mathbf{F}^{(m,n_1,\dots,n_K)}$  are explicitly linked to the inverse of  $\mathbf{C}^{(m,n_k)T}$  up to trivial indeterminacies. Therefore, solving the problem (25) yields estimates of the factor matrices  $\mathbf{C}^{(m,n_k)}$ . Subsequently, the estimates of the factor matrices  $\mathbf{A}^{(m)}$  can be obtained. We note that *Theorem 3* extends the results obtained in step (ii) in *Subsection.III.D* for  $K = 2$  to  $K \in [2, M]$ .

We denote  $\mathbf{W}^{(m,n_1,\dots,n_K)} \triangleq [\mathbf{w}_1^{(m,n_1,\dots,n_K)}, \dots, \mathbf{w}_R^{(m,n_1,\dots,n_K)}] \in \mathbb{C}^{R^k \times R}$ , and  $\mathcal{W}^{(m,n_1,\dots,n_K)} \triangleq \text{Ten}(\mathbf{W}^{(m,n_1,\dots,n_K)}, [R, R, \dots, R]) \in \mathbb{C}^{R^k \times \dots \times R}$ . According to (25),  $\mathcal{W}^{(m,n_1,\dots,n_K)}$  admits the following  $(K+1)$ th-order CPD for fixed  $m, n_1, \dots, n_K$ :

$$\mathcal{W}^{(m,n_1,\dots,n_K)} = \left[ \mathbf{B}^{(m,n_1)}, \dots, \mathbf{B}^{(m,n_K)}, \mathbf{F}^{(m,n_1,\dots,n_K)} \right]_R, \quad (26)$$

where all the factor matrices  $\mathbf{B}^{(m,n_k)}, \mathbf{F}^{(m,n_1,\dots,n_K)}$  have full column rank,  $k = 1, \dots, K$ . Hence, for all the possible values of  $1 \leq m \leq M$  and  $1 \leq n_1 < \dots < n_K \leq M$ , (26) is a  $(K+1)$ th-order overdetermined C-CPD with coupling in the first  $K$  modes.

(iii) Solve the overdetermined  $(K+1)$ th-order C-CPD (26), and calculate factor matrices  $\mathbf{A}^{(1)}, \dots, \mathbf{A}^{(M)}$ .

When  $K = 2$ , (26) is equivalent to (18) and we can use the strategy explained in step (iii) of *Subsection III. D.* for its computation. When  $K > 2$ , the tensor  $\mathcal{W}^{(m,n_1,\dots,n_K)}$  in (26) has order  $(K+1) > 3$ . We now follow [51], which explains that, under conditions that are satisfied in our derivation, the CPD of a tensor of order higher than three can equivalently be expressed as a C-CPD of third-order tensors obtained by combining modes. This C-CPD can be computed by a GEVD. Therefore, any of the  $(K+1)$ th-order CPDs can be computed by GEVD, which yields us the factor matrices  $\mathbf{B}^{(m,n_1)}, \dots, \mathbf{B}^{(m,n_K)}$ , for any choice of  $(m, n_1, \dots, n_K)$ . Then we work analogously with (19) and (20) to obtain all the factor matrices  $\mathbf{B}^{(m,n)}$ ,  $m, n = 1, \dots, M$ . The details of this procedure are given in the *Supplementary materials*.

As in the case  $K = 2$ , we may consider computing the C-CPD of all the tensors  $\mathcal{W}^{(m,n_1,\dots,n_K)}$  in (26) simultaneously via an optimization algorithm, taking the coupling into account.

Once C-CPD (26) has been computed, we calculate  $\tilde{\mathbf{C}}^{(m,n)} = \mathbf{C}^{(m,n)} \mathbf{D}_C^{(m,n)} \mathbf{\Pi} = \mathbf{B}^{(m,n)T}$ . Then, for each  $r \in [1, R]$ , we construct a set of  $N \times N$  matrices  $\mathbf{G}_r^{(m,n)} \triangleq \text{unvec}(\mathbf{T}_3^{(m,n)} \mathbf{B}^{(m,n)})_{(c,r)}$ ,  $1 \leq m, n \leq M$  and collect them in a  $NM \times NM$  matrix  $\mathbf{G}_r$  according to (21). We can calculate  $[\tilde{\mathbf{a}}_r^{(1)T}, \dots, \tilde{\mathbf{a}}_r^{(M)T}]^T$  as the dominant eigenvector of  $\mathbf{G}_r$ . Table II summarizes the algebraic algorithm in the general case.

#### F. Remarks

We present some remarks to provide insights into the theoretical and practical aspects of DC-CPD.

*Remark 3: Theorem 2 and 3* have provided deterministic uniqueness conditions under which DC-CPD can be calculated algebraically, for  $K = 2$  and  $K \in [2, M]$ , respectively. We can also provide the generic value of the upper bound of  $R$ , denoted as  $R_{\max}$ . We call a property generic if it holds with probability one, when the parameters it involves are drawn from continuous probability densities. Generically, the matrix

$\mathbf{C}^{(m,n)} \in \mathbb{C}^{R \times R}$  has full column rank. Hence, the generic version of the uniqueness conditions in *Theorem 2* and *3* depends only on  $N$ . We give the generic value of  $R_{\max}$ , for a number of different  $N$ , for  $K = 2$  and  $K = 3$ , respectively, in Table III. For comparison, we also list the generic value of  $R_{\max}$  for CPD for  $K = 2$  [10], and  $K = 3$  [13], respectively.

TABLE II  
DC-CPD: ALGEBRAIC ALGORITHM,  $2 \leq K \leq M$

Input: $\{\mathcal{T}^{(m,n)} \in \mathbb{C}^{N \times \dots \times R} \mid 1 \leq m, n \leq M\}$ admitting DC-CPD (7).	
1:	Group $\mathcal{T}^{(m,n)}$ into $M$ sets $\Upsilon^{(m)}$ by (8), and select $K \in [2, M]$ .
2:	For each combination of $K$ tensors in $\Upsilon^{(m)}$ perform the operation (13) for all the frontal slices of these tensors by (22)–(24), to construct a matrix $\mathbf{F}(\mathcal{T}^{(m,n_1)}, \dots, \mathcal{T}^{(m,n_K)})$ .
3:	Calculate the basis vectors $\mathbf{w}_r^{(m,n_1,\dots,n_K)}$ , $r = 1, \dots, R$ , of the null space of $\mathbf{F}(\mathcal{T}^{(m,n_1)}, \dots, \mathcal{T}^{(m,n_K)})$ . For varying $(m, n_1, \dots, n_K)$ , convert all the basis vectors $\mathbf{w}_r^{(m,n_1,\dots,n_K)}$ into an overdetermined C-CPD (26).
4:	Compute the nonsingular matrices $\mathbf{B}^{(m,n)}$ by solving the C-CPD (26), and then we have $\tilde{\mathbf{C}}^{(m,n)} = \mathbf{B}^{(m,n)T}$ , $\tilde{\mathbf{A}}^{(m)} \odot \tilde{\mathbf{A}}^{(n)^*} = \mathbf{T}_3^{(m,n)} \mathbf{B}^{(m,n)}$ .
5:	Compute matrix $\mathbf{G}_r$ by (21). Then the $r$ th column of the factor matrices $\tilde{\mathbf{A}}^{(m)}$ can be computed as the dominant eigenvector of $\mathbf{G}_r$ , $m = 1, \dots, M$ , $r = 1, \dots, R$ .
Output: Estimates of the factor matrices $\tilde{\mathbf{A}}^{(m)}$ and $\tilde{\mathbf{C}}^{(m,n)}$ , $1 \leq m, n \leq M$ .	

TABLE III  
GENERIC VALUE OF  $R_{\max}$  OF DC-CPD AND CPD ( $K = 2, 3$ )

$N$	2	3	4	5	6
DC-CPD ( $K = 2$ )	2	5	10	16	23
DC-CPD ( $K = 3$ )	2	6	11	18	27
CPD ( $K = 2$ )	2	4	9	14	21
CPD ( $K = 3$ )	2	4	9	16	24

The numerical values of  $R_{\max}$  can be easily obtained using *Theorem 2* and *3*, and Fisher's lemma (Corollary in p.10 of [65]). Fisher's lemma implies that, for fixed  $N$  and  $R$ , DC-CPD is generically unique if we can find one example for which the decomposition is unique. Hence, in the case  $K = 2$ , one only needs to check if the vectors  $\Psi(\mathbf{a}_t^{(m)} \mathbf{a}_t^{(p)H}, \mathbf{a}_r^{(m)} \mathbf{a}_r^{(q)H})$  are linearly independent for  $1 \leq t \neq r \leq R$ , for a set of randomly generated factor matrices  $\mathbf{A}^{(1)}, \dots, \mathbf{A}^{(M)}$ . Analogously, we can calculate the generic value of  $R_{\max}$ , for  $K \in [2, M]$ , by checking if the matrix  $\Phi_{m_1, \dots, m_K}^{(m)}$  has full column rank for a set of randomly generated factor matrices  $\mathbf{A}^{(m)}$ ,  $m = 1, \dots, M$ .

We note that the uniqueness condition depends on the preset constant  $K$ . We have generally observed that increasing  $K$  relaxes the uniqueness condition of DC-CPD. For instance, Table I shows that for  $K = 3$ , a more relaxed generic uniqueness condition is obtained than for  $K = 2$ . We have also observed that the uniqueness condition of DC-CPD for  $K = 2$  and  $K = 3$  is more relaxed than that of CPD for  $K = 2$  and  $K = 3$ , respectively. Instead of giving a formal proof, we limit ourselves to the following explanation. First, recall that  $\Phi_{n_1, \dots, n_K}^{(m)}$  has  $\Psi(\mathbf{a}_{r_1}^{(m)} \mathbf{a}_{r_1}^{(n_1)H}, \dots, \mathbf{a}_{r_K}^{(m)} \mathbf{a}_{r_K}^{(n_K)H})$  as its columns, and (13) shows that  $\Psi(\mathbf{a}_{r_1}^{(m)} \mathbf{a}_{r_1}^{(n_1)H}, \dots, \mathbf{a}_{r_K}^{(m)} \mathbf{a}_{r_K}^{(n_K)H})$  is obtained by concatenation of sub-vectors  $\text{vec}(\Phi_{(v,w)}^{(m)}(\mathbf{a}_{r_1}^{(m)} \mathbf{a}_{r_1}^{(n_1)H}, \dots, \mathbf{a}_{r_K}^{(m)} \mathbf{a}_{r_K}^{(n_K)H}))$ . The latter are obtained using the coupled rank-1 detection mapping defined in (12),  $1 \leq v < w \leq K$ . From (12) we have:



$$\begin{aligned} & \text{vec}(\Phi_{(v,w)}(\mathbf{a}_{r_1}^{(m)} \mathbf{a}_{r_1}^{(n_1)H}, \dots, \mathbf{a}_{r_K}^{(m)} \mathbf{a}_{r_K}^{(n_K)H})) \\ &= \left[ \left( \bigotimes_{k=1}^K \mathbf{a}_{r_k}^{(m)} \right) - \left( \bigotimes_{k \in \Xi_{(v,w)}} \mathbf{a}_{r_k}^{(m)} \right) \right] \otimes \left( \bigotimes_{l=1}^K \mathbf{a}_{u_l}^{(n_l)*} \right), \end{aligned}$$

where  $\Xi_{(v,w)} = \{1, \dots, v-1, w, v+1, \dots, w-1, v, w+1, \dots, K\}$ . This equation shows that  $\text{vec}(\Phi_{(v,w)}(\mathbf{a}_{r_1}^{(m)} \mathbf{a}_{r_1}^{(n_1)H}, \dots, \mathbf{a}_{r_K}^{(m)} \mathbf{a}_{r_K}^{(n_K)H}))$  is a sum of two vectors that have a Kronecker product structure. One can expect that in matrices with such Kronecker product structured columns, the likelihood of *linear* dependencies between columns will decrease as the number of factors  $2K$  increases. Second, we note that when  $K$  increases, the number of rows of  $\Phi_{(v,w)}^{(m)}$  increases faster than the number of columns. (Note that the size of  $\Phi_{(v,w)}^{(m)}$  is  $C_K^2 N^{2K} \times (R^K - R)$ ). Hence, one can again expect a more relaxed uniqueness condition for larger  $K$ . In particular, the most relaxed uniqueness condition can be expected for  $K = M$ , which implies that the coupled rank-1 detection mapping in (22) involves all the tensors in set  $\Upsilon^{(m)}$ . On the other hand, the size of  $\Gamma^{(m, n_1, \dots, n_K)}$  is  $C_K^2 N^{2K} \times R^K$ , i.e., it depends exponentially on  $K$  such that increasing  $K$  increases the computational complexity significantly. For instance, for a DC-CPD with  $N = 6$ ,  $R = 23$ , and  $M = 3$ , the matrix  $\Gamma^{(m, n_1, \dots, n_K)}$  has size  $1296 \times 529$  for  $K = 2$ , and has size  $139968 \times 12167$  for  $K = 3$ . As such, if in a practical application uniqueness does not have to be ensured for a very high number of sources, we may limit ourselves to the minimal value  $K = 2$  for efficiency of computation.

*Remark 4:* The algebraic DC-CPD approach is guaranteed to return the exact solution in the exact case. When noise is present, the conventional linear algebra operations, such as the calculation of the basis vectors of the null space of a matrix as its singular vectors, and the matrix best rank-1 approximation, are by themselves optimal in LS sense. The overall result, however, is not guaranteed to be optimal and is actually (mildly) suboptimal in practice. To estimate the optimal result, we can fit the DC-CPD in LS sense by an optimization algorithm, e.g. via the implementation with SDF, or by using the ALS scheme.

Note that an optimization based DC-CPD algorithm, which directly maximize the fit of the data tensors, provides the optimal results in the LS sense, if it converges to the global minimum. However, we have observed that in J-BSS, especially in underdetermined J-BSS, the optimization based DC-CPD algorithms are very sensitive to initialization, and sometimes do not return the correct results even in the noiseless case. Therefore, in practice, we can use the algebraic algorithm to efficiently initialize the optimization based algorithms.

*Remark 5:* By definition, DC-CPD consists of a set of CPDs with coupled factors. One can obviously compute each CPD and consider these individual CPD solutions as the solution to DC-CPD. It is then natural to ask what benefits DC-CPD have over CPD. We briefly mention the following.

First, DC-CPD is able to provide better robustness to noise and model errors than CPD as it exploits more information and the way it is coupled. As in J-BSS, the coupling comes from the similarity of the sources across different datasets, DC-CPD is expected to perform well in finding components that are

consistently present in multi-set signals. Second, DC-CPD components from distinct datasets are automatically aligned. In other words, DC-CPD avoids the permutation alignment / parameter pairing in a post-processing step, which can otherwise be difficult and time-consuming. Third, DC-CPD can be unique when none of its constituting CPDs is unique.

*Remark 6:* We note that the main complexity of the algebraic DC-CPD algorithm, as it has been presented, is in the construction of matrices  $\Gamma^{(m, n_1, \dots, n_K)}$  and the calculation of the basis vectors in their null space. We have according to (12) and (13), that the complexity of the construction of each column of  $\Gamma^{(m, n_1, \dots, n_K)}$  is  $O(C_K^2 KN^{2K})$  flops, and thus the overall complexity of the construction of  $\Gamma^{(m, n_1, \dots, n_K)}$  is  $O(C_K^2 KN^{2K} R^K)$  flops. The basis vectors in  $\ker(\Gamma^{(m, n_1, \dots, n_K)})$  are computed as singular vectors. This step has complexity  $O(2C_K^2 N^{2K} R^{2K} + 11R^{3K})$  flops. We construct and manipulate  $MC_M^K$  such matrices  $\Gamma^{(m, n_1, \dots, n_K)}$ . Therefore, the overall complexity is  $O(MC_M^K (C_K^2 KN^{2K} R^K + 2C_K^2 N^{2K} R^{2K} + 11R^{3K}))$  flops. The memory requirements of the algorithm are mainly in the storage of the  $MC_M^K$  tensors  $\mathcal{W}^{(m, n_1, \dots, n_K)}$  and the matrix  $\Gamma^{(m, n_1, \dots, n_K)}$ . Therefore, the memory requirements are  $O(MC_M^K (R^{(K+1)} + C_K^2 N^{2K} R^K))$  complex numbers. In the simplest case  $K = 2$ , the complexity is  $O(M^3 N^4 R^2 + M^3 N^4 R^4 + 5.5M^3 R^6)$  flops. The memory requirements are  $O(0.5M^3 R^3 + 0.5M^3 N^4 R^2)$  complex numbers.

However, the algebraic DC-CPD admits an efficient implementation. Instead of explicitly constructing  $\Gamma^{(m, n_1, \dots, n_K)}$ , we can calculate the  $R^K \times R^K$  Hermitian matrices  $\mathbf{\Omega}^{(m, n_1, \dots, n_K)} \triangleq \Gamma^{(m, n_1, \dots, n_K)H} \Gamma^{(m, n_1, \dots, n_K)}$ , taking advantage of the algebraic structure of  $\Gamma^{(m, n_1, \dots, n_K)}$ . We note that  $\ker(\mathbf{\Omega}^{(m, n_1, \dots, n_K)}) = \ker(\Gamma^{(m, n_1, \dots, n_K)})$ , while  $\mathbf{\Omega}^{(m, n_1, \dots, n_K)}$  have smaller size and can be computed more efficiently than  $\Gamma^{(m, n_1, \dots, n_K)}$ . We provide the details in the *Supplementary materials*. Compared with the original version of algebraic DC-CPD, this implementation has lower complexity and memory requirements, namely  $O(0.5MC_M^K C_K^2 N^2 R^{2K} + 2MC_M^K R^{3K})$  flops and  $O(M^2 N^2 R^2 + MC_M^K R^{2K})$  complex numbers, respectively. In the simplest case  $K = 2$ , the complexity and memory requirements of this efficient implementation are  $O(0.5M^3 N^2 R^4 + M^3 R^6)$  flops and  $O(M^2 N^2 R^2 + 0.5M^3 R^4)$  complex numbers, respectively. Although the complexity may seem a lot at first sight, it is actually quite reasonable. Recall from *Subsection III. A*, that in the algebraic underdetermined framework, all problems are transformed into overdetermined problems via the computation of the null space of a matrix that has at least  $O(R^2)$  columns. In numerical linear algebra, factorizations of  $M \times N$  matrices typically have a complexity proportional to  $O(MN^2)$  [66]. In this perspective, the complexity of the efficient implementation is indeed very reasonable. Note that the efficient implementation has exploited the full coupling structure, i.e. we did not sacrifice part of the available information to gain in terms of speed.

Note that  $N < R$  in the above expressions. When  $N \geq R$ , there is no need to use the coupled rank-1 detection mapping, and the complexity is equal to that of a GEVD based scheme,

which is much lower.

We note that the complexity and memory requirements of the proposed algebraic DC-CPD are jointly determined by  $N, K, R, M$ . In practice, computational resources are often limited, and we can make the following additional remarks on the efficiency of proposed algorithm in J-BSS.

(i) We can limit ourselves to the minimal value  $K = 2$  if uniqueness does not have to be ensured for a very large value of  $R$ .

(ii) If  $N > R$ , dimensionality reduction needs to be performed before J-BSS. This does not only reduce the value of  $N$ , but also suppresses the noise.

(iii) A point of attention is that in applications that involve many datasets, often only a few of them are highly correlated. We should only construct the cross-covariance tensors for datasets that are sufficiently correlated. This reduces the complexity ( $M$  is de facto small) and also guarantees that the constructed data tensors have a sufficiently high signal-to-noise ratio (SNR).

(iv) In our derivation, we have exploited the full coupling structure. In practice, we may consider using partial structure to reduce the complexity. In particular, the complexity can be reduced by (1) reducing the size of  $\mathbf{F}^{(m, n_1, \dots, n_K)}$ , and/or by (2) reducing the number of matrices  $\mathbf{F}^{(m, n_1, \dots, n_K)}$ . We first explain how to reduce the size of  $\mathbf{F}^{(m, n_1, \dots, n_K)}$ . As shown in *Theorem 3*, what is crucial to the derivation of the algebraic DC-CPD algorithm, is that we obtain a set of linearly independent vectors  $\psi(\mathbf{a}_{r_1}^{(m)} \mathbf{a}_{r_1}^{(n_1)H}, \dots, \mathbf{a}_{r_K}^{(m)} \mathbf{a}_{r_K}^{(n_K)H})$ , where each tuple  $(r_1, \dots, r_K)$  has at least two distinct elements. In definition (13), the vector  $\psi(\mathbf{X}^{(1)}, \dots, \mathbf{X}^{(K)})$  is defined through concatenation of the subvectors obtained by applying the coupled rank-1 detection mapping to all pairs of matrices. This full exploitation of the coupling structure makes it the most likely that the set of vectors  $\psi(\mathbf{a}_{r_1}^{(m)} \mathbf{a}_{r_1}^{(n_1)H}, \dots, \mathbf{a}_{r_K}^{(m)} \mathbf{a}_{r_K}^{(n_K)H})$  are linearly independent, while it also yields the highest complexity. In practice, we may compute only part of the entries of  $\psi(\cdot)$ . The algorithm will work as long as the vectors  $\psi(\mathbf{a}_{r_1}^{(m)} \mathbf{a}_{r_1}^{(n_1)H}, \dots, \mathbf{a}_{r_K}^{(m)} \mathbf{a}_{r_K}^{(n_K)H})$  are linearly independent. By way of example, if we apply the coupled rank-1 detection mapping only to combinations of  $\mathbf{X}^{(1)}$  and one of the other matrices  $\mathbf{X}^{(2)}, \dots, \mathbf{X}^{(K)}$ , then that will reduce the length of  $\psi(\mathbf{X}^{(1)}, \dots, \mathbf{X}^{(K)})$  to  $(K-1)N^K \prod_{k=1}^K J_k$ .

Another way to reduce the complexity is to reduce the number of matrices. More precisely, the matrices  $\mathbf{F}^{(m, n_1, \dots, n_K)}$  are obtained by exploiting the coupling between all the  $K$  combinations of coupled tensors in the original DC-CPD (8). In practice, we may consider exploiting the coupling between tensors  $\mathcal{T}^{(m,1)}, \dots, \mathcal{T}^{(m,K-1)}$  and each of the remaining tensors  $\mathcal{T}^{(m,K)}, \dots, \mathcal{T}^{(m,M)}$ , for each fixed  $m$ . That will result in a reduced number of  $M(M-K+1)$  tensors  $\mathcal{W}^{(m, n_1, \dots, n_K)}$  in (26).

#### IV. EXPERIMENTS

In this section we present experiment results to demonstrate the performance of DC-CPD, in comparison with standard CPD. In experiment A, we discuss high-accuracy computation of exact decompositions. In experiment B, we compare DC-CPD and other BSS or J-BSS algorithms in J-BSS of synthetic noisy

multi-set signals. In experiment C, we apply DC-CPD in wide-band array signal direction-of-arrival (DOA) estimation. In experiment B and C, we consider both overdetermined and underdetermined cases.

We use the following abbreviations:

- DC-CPD-ALG: algebraic DC-CPD algorithm.
- DC-CPD-ALS: DC-CPD via ALS.
- DC-CPD-SDF: DC-CPD via SDF.
- SOBIUM: second-order blind identification of underdetermined mixtures [11]. It is based on the CPD of the auto-covariance tensor for each dataset.
- CPD-C: variant of SOBIUM based on the CPD of the cross-covariance tensor of two datasets. It can be considered as a J-BSS algorithm for two datasets.
- M-CCA: multi-set canonical covariance analysis [33].
- GOJD: generalized orthogonal joint diagonalization of second-order cross-covariance matrices between multiple prewhitened datasets [37].

DC-CPD-SDF is implemented using the ‘sdf\_nls.m’ function in Tensorlab 3.0 [64]. In the implementation of DC-CPD-ALG, we use the SD based scheme to solve the overdetermined C-CPD in (18) or (26). In the implementation of DC-CPD-ALS and DC-CPD-SDF, we initialize either randomly or by the results of DC-CPD-ALG, depending on the application. The initialization details will be given in each of the following examples. In the implementation of SOBIUM and CPD-C, we use the ‘cpd.m’ function with default setting<sup>1</sup> in Tensorlab 3.0 for the CPD that they involve. In experiments B and C, the data tensors  $\mathcal{T}^{(m,n)}$  in (3) are approximated by their finite-sample version:

$$\left(\tilde{\mathcal{T}}^{(m,n)}\right)_{(:,i:,k)} = L^{-1} \cdot \left[ \sum_{l=1}^L \left(\mathbf{X}^{(m,k)}\right)_{(:,l)} \left(\mathbf{X}^{(n,k)}\right)_{(:,l)}^H \right], \quad (27)$$

where  $\mathbf{X}^{(m,k)} \in \mathbb{C}^{N \times L}$  denotes the  $k$ th temporal frame of  $\mathbf{x}^{(m)}(t)$  in (3) with frame length  $L$ , overlapping with adjacent frames with overlap ratio  $\alpha \in [0, 1]$ .

In experiment C, we use the benchmark codes ‘stft.m’ and ‘istft.m’ from [67] to perform the short-time Fourier transform (STFT) and the inverse STFT (ISTFT). All the experiments are performed on a computer with following configuration, CPU: Intel Core i7-4930MX 3.0GHz; Memory: 32GB; System: 64bit Windows 7; MATLAB R2013b.

##### A. Results for exact decompositions

The data tensors are directly generated by (4), where both the real and imaginary parts of each entry of the factor matrices  $\mathbf{A}^{(m)} \in \mathbb{C}^{N \times R}$  and  $\mathbf{C}^{(m,n)} \in \mathbb{C}^{R \times R}$  are randomly drawn from a standard normal distribution, and no noise is added. We fix the third dimension of all the data tensors to  $R$  and let the number of

<sup>1</sup> The default setting of ‘cpd.m’ in Tensorlab 3.0 is: (i) If the rank of a tensor is smaller than its first two dimensions, then a GEVD based initialization is used, otherwise a random initialization is used with entries drawn from the normal distribution; (ii) A Gauss-Newton based optimization algorithm is used to compute the CPD. This algorithm is implemented in ‘cpd\_nls.m’. The tolerance on the relative function value and the tolerance on the relative step size in the stopping criteria are set to TolFun =  $10^{-12}$  and TolX =  $10^{-8}$ , respectively.

mixing matrices  $M=4$ . The mean relative error of the estimates of all the loading matrices is defined as:

$$\varepsilon = M^{-1} \sum_{m=1}^M \min_{\mathbf{I}^{(m)}, \mathbf{D}^{(m)}} \left( \left\| \mathbf{A}^{(m)} - \mathbf{I}^{(m)} \mathbf{D}^{(m)} \tilde{\mathbf{A}}^{(m)} \right\|_F^2 / \left\| \mathbf{A}^{(m)} \right\|_F^2 \right), \quad (28)$$

where  $\tilde{\mathbf{A}}^{(m)}$  is the estimate of the true mixing matrix  $\mathbf{A}^{(m)}$ ,  $\mathbf{I}^{(m)}$  is a permutation matrix and  $\mathbf{D}^{(m)}$  is a diagonal matrix. For DC-CPD-ALS and DC-CPD-SDF, we try ten random initial values and select the one that gives the best fit after the first ten iterations to effectively initialize the algorithm. As there is no noise, we want to estimate the factor matrices with high precision. Therefore, we terminate the ALS iteration when  $|\xi_{cur} - \xi_{prev}| / \xi_{prev} \leq 10^{-12}$ , where  $\xi_{cur}$  and  $\xi_{prev}$  denote the LS error in the current and previous iteration, respectively. For DC-CPD-SDF, we set the termination parameters ‘TolFun’ and ‘TolX’ in ‘sdf\_nls.m’ to  $10^{-12}$  and  $10^{-6}$ , respectively. In addition, we set the maximal number of iterations to 1000 for both DC-CPD-ALS and DC-CPD-SDF. The mean relative error and CPU time (denoted as ‘ $t$ ’) of DC-CPD-ALG, DC-CPD-ALS and DC-CPD-SDF for different values of  $N$  and  $R$  are reported in Table IV. Note that, under the listed conditions, the rank  $R$  is high and CPD has been proven to be generically not unique [18]. The average number of iterations of DC-CPD-ALS and DC-CPD-SDF (denoted as ‘ $it$ ’), and the order of the coupled rank-1 detection mapping used in DC-CPD-ALG (denoted as ‘ $K$ ’) are also reported in Table IV. We select  $K$  as the minimal number for which DC-CPD-ALG finds the correct solution. All the results in Table IV are averaged over 100 independent runs.

TABLE IV

PERFORMANCE OF DC-CPD-ALG, DC-CPD-ALS, DC-CPD-SDF IN EXACT DECOMPOSITIONS. ‘ $N$ ’ IS THE NUMBER OF OBSERVATIONS, ‘ $R$ ’ IS THE NUMBER OF SOURCES, ‘ $\varepsilon$ ’ IS THE MEAN RELATIVE ERROR, ‘ $t$ ’ IS THE MEAN CPU TIME, ‘ $K$ ’ IS THE ORDER OF THE COUPLED RANK-1 DETECTION MAPPING IN DC-CPD-ALG, AND ‘ $it$ ’ IS THE AVERAGE NUMBER OF ITERATIONS FOR DC-CPD-ALS AND DC-CPD-SDF

	DC-CPD-ALG	DC-CPD-ALS	DC-CPD-SDF
$N=3$	$\varepsilon = 2.14 \times 10^{-11}$	$\varepsilon = 3.83 \times 10^{-10}$	$\varepsilon = 2.07 \times 10^{-7}$
$R=5$	$t = 0.39$ sec.	$t = 9.48$ sec.	$t = 12.47$ sec.
	$K=2$	$it = 693$	$it = 174$
$N=3$	$\varepsilon = 1.98 \times 10^{-12}$	$\varepsilon = 0.106$	$\varepsilon = 0.230$
$R=6$	$t = 1.50$ sec.	$t = 13.55$ sec.	$t = 73.52$ sec.
	$K=3$	$it = 1000$	$it = 929$
$N=4$	$\varepsilon = 2.36 \times 10^{-12}$	$\varepsilon = 0.079$	$\varepsilon = 0.0013$
$R=10$	$t = 3.09$ sec.	$t = 16.73$ sec.	$t = 71.36$ sec.
	$K=2$	$it = 1000$	$it = 793$
$N=4$	$\varepsilon = 2.04 \times 10^{-11}$	$\varepsilon = 0.3622$	$\varepsilon = 0.4547$
$R=11$	$t = 40.21$ sec.	$t = 19.82$ sec.	$t = 95.22$ sec.
	$K=3$	$it = 1000$	$it = 1000$

We observe that in all the considered cases, DC-CPD-ALG has found the exact solution. DC-CPD-ALS and DC-CPD-SDF, however, did not always find the correct solution in the last three cases, even in the absence of noise. This can be seen from the histograms of the mean relative errors of DC-CPD-ALS and DC-CPD-SDF (By way of example, the histogram for setting  $N=3, R=6$  is shown in Fig. 2). Further, Table IV shows that DC-CPD-ALG provides more efficient computation than DC-CPD-ALS and DC-CPD-SDF in exact decompositions. In

practice, noise is usually present, and the performance of DC-CPD-ALG will deteriorate, but can still be used as a low-cost initialization for DC-CPD-ALS and DC-CPD-SDF, which directly fit the data tensor in the LS sense. This will be shown later.

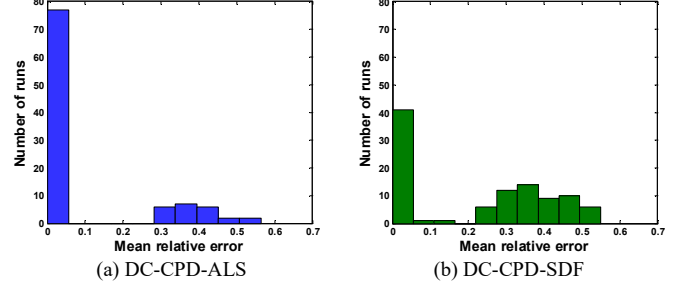


Fig. 2. Histogram of mean relative error for DC-CPD-ALS and DC-CPD-SDF in experiment A.  $N=3, R=6$ .

### B. J-BSS of multi-set signals

In this experiment we use the finitely sampled version of the multi-set data model (2). The number of samples in each dataset is denoted as  $Q$ . We generate the  $Q \times R$  source matrix  $\mathbf{S}^{(m)}$  from auxiliary matrix  $\mathbf{S}'_r$  of size  $Q \times M$  as follows:

$$\mathbf{S}'_r = \mathbf{Q}_r \mathbf{S}'_r{}^T, \quad (29)$$

where  $\mathbf{S}'_r \triangleq [(\mathbf{S}^{(1)})_{:,r}, \dots, (\mathbf{S}^{(M)})_{:,r}] \in \mathbb{C}^{Q \times M}$ ,  $(\mathbf{S}^{(m)})_{:,r}$  denotes the  $r$ th source vector in the  $m$ th dataset and  $\mathbf{Q}_r \in \mathbb{C}^{M \times M}$  is a full rank matrix used to introduce inter-set dependence between the corresponding source signals in different datasets. Both the real and imaginary part of each entry of  $\mathbf{Q}_r$  are drawn from a standard normal distribution. The underlying generating source matrix  $\mathbf{S}'_r(t) \triangleq [s'_{r,1}(t), \dots, s'_{r,M}(t)]$  consists of complex binary phase shift keying (BPSK) signals that are amplitude modulated across  $P$  time slots of length  $L'$ :

$$\mathbf{s}'_r{}^T(t) = [\eta_1 \cdot s'_{r,1}(t)^T, \dots, \eta_P \cdot s'_{r,P}(t)^T]^T \in \mathbb{C}^Q, \quad (30)$$

where  $\eta_1, \dots, \eta_P$  are amplitude modulation coefficients that are randomly drawn from a uniform distribution over  $[0, 1]$ , and where  $Q = PL'$ . The sub-vector  $\mathbf{s}'_{r,p}(t)$  of length  $L'$  is a complex BPSK sequence with entries chosen from symbols  $[1, -1]$  with equal probability. By definition,  $\mathbf{s}'_r{}^T(t)$  is the concatenation of  $P$  BPSK sequences, the amplitudes of which have been modulated by coefficients  $\eta_1, \dots, \eta_P$ . In this experiment,  $P$  is fixed to 20 and  $L' = Q/20$ .

The mixtures are constructed as:

$$\mathbf{X}^{(m)} = \sigma_s \frac{\mathbf{A}^{(m)} \mathbf{S}^{(m)T}}{\|\mathbf{A}^{(m)} \mathbf{S}^{(m)T}\|_F} + \sigma_n \frac{\mathbf{N}^{(m)}}{\|\mathbf{N}^{(m)}\|_F}, \quad m=1, \dots, M, \quad (31)$$

where the real and imaginary part of each entry of  $\mathbf{A}^{(m)}$  are drawn from a standard normal distribution. Matrix  $\mathbf{N}^{(m)}$  denotes the white Gaussian noise term added in the  $m$ th dataset, and  $\sigma_s, \sigma_n$  denote the signal level and noise level, respectively. The SNR is defined as:

$$\text{SNR} = 20 \log_{10}(\sigma_s / \sigma_n). \quad (32)$$

DC-CPD-ALS and DC-CPD-SDF are initialized with the results of DC-CPD-ALG. The ALS iteration in DC-CPD-ALS

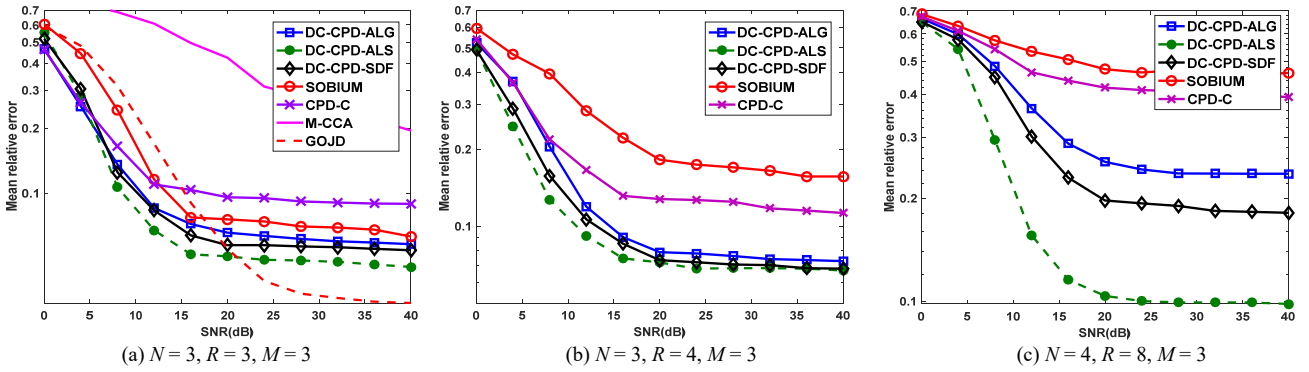


Fig. 3. Mean relative error of DC-CPD-ALG, DC-CPD-ALS, DC-CPD-SDF, SOBIUM, and CPD-C vs. SNR in experiment B. The plots illustrate the performance in (a) an overdetermined setting, (b) a slightly underdetermined setting, and (c) a highly underdetermined setting. In setting (a) M-CCA and GOJD are also included in the comparison.

is terminated when  $|\xi_{cur} - \xi_{prev}| / \xi_{prev} \leq 10^{-6}$ . The termination parameters ‘TolFun’ and ‘TolX’ of the ‘sdf\_nls.m’ function used in DC-CPD-SDF are set to  $10^{-6}$  and  $10^{-3}$ , respectively. The order of the coupled rank-1 detection mapping used in DC-CPD-ALG is fixed to its minimum value  $K = 2$ .

We demonstrate the performance of the compared methods in the following three settings: (a) an overdetermined case  $N = 3, R = 3, M = 3$ ; (b) a slightly underdetermined case  $N = 3, R = 4, M = 3$ , and (c) a highly underdetermined case  $N = 4, R = 8, M = 3$ . In setting (a), we fix the number of snapshots  $Q = 1000$ , the framelength  $L = 50$ , the overlap ratio  $\alpha = 0.5$ , the number of frames  $T = 39$ . In setting (b), we set  $Q = 2000, L = 100, \alpha = 0.5, T = 39$ . In setting (c), we set  $Q = 5000, L = 250, \alpha = 0.5, T = 39$ . In all the three settings, DC-CPD-ALG, DC-CPD-ALS, DC-CPD-SDF, SOBIUM, and CPD-C are performed. M-CCA and GOJD are performed only in setting (a) as they are algorithms for overdetermined J-BSS. We provide more results, with different parameters  $Q, L, T, M$ , in the *Supplementary materials*. The results are in general consistent with those shown here, and they give additional insight in how the performance of different methods depends on these parameters.

We let SNR vary from 0dB to 40dB. The mean relative error  $\varepsilon$  versus SNR is plotted in Fig. 3 to illustrate the performance of the compared algorithms in the three settings. We perform 200 Monte Carlo runs to calculate each point in the curves. We can clearly see from Fig. 3 that all the DC-CPD algorithms perform better than both SOBIUM and CPD-C in all the three settings, as they use the information in both the auto-covariance and cross-covariance tensors, as well as the way the tensors are coupled. SOBIUM and CPD-C, on the other hand, use only auto-covariance or cross-covariance tensors. In setting (a), we see that all the DC-CPD algorithms perform better than M-CCA for all SNR levels. They perform better than GOJD for low SNR (0dB–20dB), and slightly worse than the latter for high SNR (20dB–40dB). The good performance of GOJD at high SNR is mainly the result of prewhitening, which is possible only in the overdetermined case.

In addition, we observe that DC-CPD-ALS and DC-CPD-SDF yield more accurate results than DC-CPD-ALG. This shows that DC-CPD-ALS and DC-CPD-SDF, which directly

optimize the LS cost function are more accurate than DC-CPD-ALG in the presence of noise and errors caused by finite sample effects. Overall, the difference is not very large. As expected, it is more significant when the problem is more challenging.

Comparing the results in the three settings, including those in the *Supplementary materials*, we note that the J-BSS problem itself gets more sensitive to noise and model errors (e.g. finite sampling errors) when it becomes more underdetermined. For example, in the overdetermined setting (a), all the DC-CPD algorithms perform well at medium and high SNR levels, even if the framelength  $L$  is as small as 50. In the slightly underdetermined setting (b), DC-CPD has comparable accuracy as in setting (a), with the framelength  $L$  increased to 100. In the highly underdetermined setting (c), the accuracy of DC-CPD is worse than in (a) and (b), even with  $L = 250$ .

### C. Wideband DOA estimation via a small scaled array

Wideband DOA estimation is a challenging problem in array processing as the conventional methods based on linear instantaneous mixing model only apply to narrowband signals. The conventional way to handle wideband signals is to transform them into multiple narrowband signals in different frequency bins, use narrowband techniques for each bin separately, and integrate these results (see [68] and references therein). In this example, we will illustrate how J-BSS can be used to fuse the signals in adjacent frequency bins to improve the performance of wideband DOA estimation. In this experiment, we will use small-scaled arrays, which are of particular interest for space-limited applications such as air-borne array processing. We mainly consider the far-field mixing model in this experiment. Note that our method does not impose any specific assumption on the structure of the mixing matrix, and thus also applies to other models. The two configurations used in this experiment are shown in Fig. 4.

The wideband array signal in the time domain is given by:

$$\mathbf{y}(t) = \sum_r \mathbf{h}_r(t) \star s_r(t) + \mathbf{n}(t), \quad (33)$$

where ‘ $\star$ ’ denotes the linear convolution,  $\mathbf{y}(t), \mathbf{n}(t) \in \mathbb{R}^N$  denote the array signal and noise term at time instance  $t$ ,  $\mathbf{h}_r(t)$  is the array impulse response for the  $r$ th source signal  $s_r(t)$  at time instance  $t$ . We assume that there are  $Q$  time samples, and



that the array impulse response has finite length  $F$ . We denote  $\mathbf{Y} \triangleq [\mathbf{y}(1), \dots, \mathbf{y}(Q)] \in \mathbb{R}^{N \times Q}$ ,  $\mathbf{N} \triangleq [\mathbf{n}(1), \dots, \mathbf{n}(Q)] \in \mathbb{R}^{N \times Q}$ ,  $\mathbf{s}_r \triangleq [s_r(1), \dots, s_r(Q)]^T \in \mathbb{R}^Q$ ,  $\mathbf{H}_r \triangleq [\mathbf{h}_r(1), \dots, \mathbf{h}_r(F)] \in \mathbb{R}^{N \times F}$ . We can rewrite (33) as:

$$\mathbf{Y} = \sum_r \mathbf{H}_r \star \mathbf{s}_r^T + \mathbf{N}. \quad (34)$$

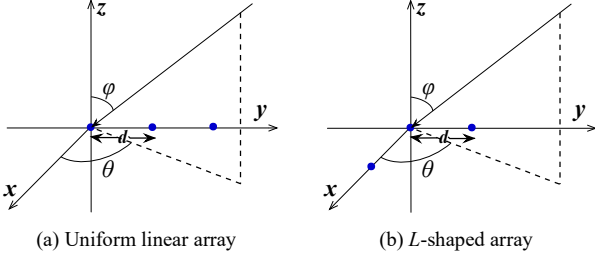


Fig. 4. Array configurations and angle definition in experiment C.

The time-frequency domain presentation of (34) is:

$$\mathbf{Y}^{(f)} = \sum_r \mathbf{a}_r^{(f)} \mathbf{s}_r^{(f)T} + \mathbf{N}^{(f)}, \quad f = 1, \dots, F, \quad (35)$$

where  $\mathbf{Y}^{(f)}$ ,  $\mathbf{N}^{(f)} \in \mathbb{C}^{N \times Q'}$  and  $\mathbf{s}_r^{(f)} \in \mathbb{C}^{Q'}$  are the narrowband component of  $\mathbf{Y}$ ,  $\mathbf{N}$  and  $\mathbf{s}_r$  in the  $f$ th frequency bin, respectively. Parameter  $Q'$  denotes the number of time samples of source component  $\mathbf{s}_r^{(f)}$  in each frequency bin. Vector  $\mathbf{a}_r^{(f)} \in \mathbb{C}^N$  contains the frequency response coefficients of  $\mathbf{H}_r$  in the  $f$ th frequency bin:

$$\mathbf{a}_r^{(f)} \triangleq \exp(-i2\pi c^{-1} f) \cdot \mathbf{K} \mathbf{p}_{(\theta_r, \varphi_r)}, \quad (36)$$

where  $\mathbf{p}_{(\theta, \varphi)} \triangleq [\cos \theta \sin \varphi, \sin \theta \sin \varphi, \cos \varphi]^T$  is the direction vector with azimuth  $\theta$  and elevation  $\varphi$  (see Fig. 4 for the definition of the angles), and  $\theta_r$  and  $\varphi_r$  are the azimuth and elevation of the  $r$ th source signal, respectively. Each row of  $\mathbf{K} \in \mathbb{R}^{3 \times 3}$  holds the Cartesian coordinates of the corresponding antenna. In particular,  $\mathbf{K} = [(0, d, 0)^T, (0, d, 0)^T, (0, d, 0)^T]^T$  for the uniform linear array (ULA) in Fig. 4 (a), and  $\mathbf{K} = [(0, d, 0)^T, (0, 0, 0)^T, (d, 0, 0)^T]^T$  for the  $L$ -shaped array in Fig. 4 (b). Parameter  $d$  denotes the interspacing between two adjacent antennas, and  $c$  denotes the wave propagation speed. Note that the wideband array signal in the time domain is real-valued, while its time-frequency presentation (35) is complex-valued.

In our experiment, we generate the wideband array signal in the time domain, according to (34). The source signal  $\mathbf{s}_r$  is generated as:  $\mathbf{s}_r = \mathbf{s}'_r \star \mathbf{s}_c \in \mathbb{R}^Q$ , where  $\mathbf{s}_c$  is a single-tone carrier signal with frequency  $f_c = 100$  MHz. The baseband signal  $\mathbf{s}'_r$  is an amplitude modulated BPSK signal constructed as in (30):  $\mathbf{s}'_r = [\eta_1 \cdot \mathbf{s}'_{r,1}, \dots, \eta_P \cdot \mathbf{s}'_{r,P}]^T \in \mathbb{R}^Q$ , where  $\eta_1, \dots, \eta_P$  are amplitude modulation coefficients that are randomly drawn from a uniform distribution over  $[0, 1]$ . The sub-vector  $\mathbf{s}'_{r,p}$  of length  $L'$  is a real-valued BPSK sequence with symbols chosen from  $[1, -1]$  with equal probability. Here  $P$  is fixed to 32 and thus  $L' = Q/32$ . For the construction of  $\mathbf{s}'_{r,p}$ , we let the bitrate  $f_b = 10$  MHz and the sampling rate  $f_s = 80$  MHz. Note that the source signals have 3dB bandwidth of approximately  $f_{bw} \approx 55$  MHz in average. They are wideband signals as their relative bandwidth is as high as  $f_{bw}/f_c \approx 0.55$ .

The impulse response matrices  $\mathbf{H}_r$  are generated as follows: First we construct  $\mathbf{A}_r \triangleq [\mathbf{a}_r^{(1)}, \dots, \mathbf{a}_r^{(F)}] \in \mathbb{C}^{N \times F}$ , with  $\mathbf{a}_r^{(f)}$

generated as in (36). Then, each row of  $\mathbf{H}_r$  is obtained by the inverse digital Fourier transform (IDFT) of the corresponding row of  $\mathbf{A}_r$ . Here we let  $F = 16$ . The noise term  $\mathbf{N}$  in the time domain is generated as a real-valued white Gaussian signal.

To construct the multi-set data for J-BSS, we convert the wideband array signal  $\mathbf{Y}$  to the time-frequency domain via STFT with frame length  $F = 16$ . By definition, the bandwidth of each frequency bin is  $f_s/F = 5$  MHz  $= 0.05 f_c$ , and thus the array signal component in each frequency bin admits the narrowband formulation (35). Note that the number of time samples in each frequency bin is  $Q' = 2Q/F = Q/8$ .

We select the signals in the fourth and fifth frequency bin as the multi-set data. The reason for this selection is that we have observed that only between two neighboring frequency bins the inter-set dependence required for J-BSS is sufficiently strong, while the selected two frequency bins account for more than 60% of the total amount of energy of the observed mixture. Denoting the selected multi-set data as  $\mathbf{x}^{(m)}(t)$ ,  $m = 1, 2$ , we have:

$$\begin{aligned} \mathbf{X}^{(1)} &= \mathbf{Y}^{(4)} = \sum_r \mathbf{a}_r^{(4)} \mathbf{s}_r^{(4)T} + \mathbf{N}^{(4)}, \\ \mathbf{X}^{(2)} &= \mathbf{Y}^{(5)} = \sum_r \mathbf{a}_r^{(5)} \mathbf{s}_r^{(5)T} + \mathbf{N}^{(5)}. \end{aligned} \quad (37)$$

We calculate by (27), for a chosen framelength  $L = Q'/32$  and overlap ratio  $\alpha = 0.5$ , the second-order covariance tensors  $\tilde{\mathcal{T}}^{(m,n)}$  with  $1 \leq m, n \leq 2$  as the data tensors for DC-CPD. We initialize DC-CPD-ALS and DC-CPD-SDF by the results of DC-CPD-ALG. The ALS iteration in DC-CPD-ALS is terminated when  $|\mathcal{E}_{cur} - \mathcal{E}_{prev}| / \mathcal{E}_{prev} \leq 10^{-12}$ . The termination parameters 'TolFun' and 'TolX' in the 'sdf\_nls.m' function used in DC-CPD-SDF are set to  $10^{-8}$  and  $10^{-4}$ , respectively. The order of the coupled rank-1 detection mapping used in DC-CPD-ALG is fixed to its minimum value  $K = 2$ . After DC-CPD or CPD has been performed to estimate  $\mathbf{a}_r^{(4)}, \mathbf{a}_r^{(5)}$ , the DOAs are estimated by solving (36). Note that the accuracy of DOA estimation depends on how well the steering vectors  $\mathbf{a}_r^{(4)}, \mathbf{a}_r^{(5)}$  are identified. We here use the mean relative estimation error, as defined in (28), to evaluate the performance of the compared algorithms.

We consider the following two cases: (a) an overdetermined setting: two sources impinge on a ULA, as shown in Fig. 4 (a), from DOAs  $(\theta_1, \varphi_1) = (45^\circ, 22.5^\circ)$ , and  $(\theta_2, \varphi_2) = (135^\circ, 67.5^\circ)$ ; (b) a highly underdetermined setting: five sources impinge on an  $L$ -shaped array, as shown in Fig. 4 (b), from DOAs  $(\theta_1, \varphi_1) = (18^\circ, 9^\circ)$ ,  $(\theta_2, \varphi_2) = (54^\circ, 27^\circ)$ ,  $(\theta_3, \varphi_3) = (90^\circ, 45^\circ)$ ,  $(\theta_4, \varphi_4) = (126^\circ, 63^\circ)$ , and  $(\theta_5, \varphi_5) = (162^\circ, 81^\circ)$ . In setting (a), the number of time samples in each frequency bin is  $Q' = 800$ . In setting (b), we fix  $Q' = 12800$ . In both cases, the interspacing  $d$  between antennas is set equal to the wavelength of the carrying wave. We include DC-CPD-ALG, DC-CPD-ALS, DC-CPD-SDF, SOBIUM, and CPD-C in the comparison. In the first case, we also include GOJD in the comparison.

The SNR is defined in (32) with  $\sigma_s$  and  $\sigma_n$  denoting the signal and noise levels in the time domain, respectively. In the experiment, we let SNR vary from 0dB to 20dB. The mean relative error of the algorithms in the above two cases is plotted

in Fig. 5.

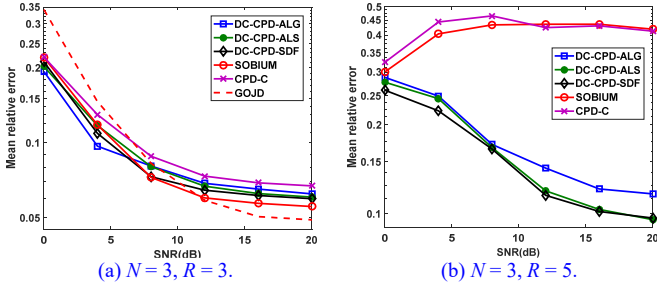


Fig. 5. Mean relative error of DC-CPD-ALG, DC-CPD-ALS, DC-CPD-SDF, SOBIUM, and CPD-C in wideband DOA estimation. The plots illustrate the performance in (a) an overdetermined setting, and (b) a highly underdetermined setting. In setting (a), GOJD is also included in the comparison.

In Fig. 5 (a) we observe that all the algorithms provide quite accurate results in the overdetermined setting. DC-CPD-ALS and DC-CPD-SDF perform about the same. Compared with DC-CPD-ALG, the additional optimization by DC-CPD-ALS and DC-CPD-SDF yields little improvement in this easy case. Comparing DC-CPD and CPD, we note that the DC-CPD algorithms perform better than CPD-C for all SNR levels. On the other hand, SOBIUM performs better than DC-CPD at high SNR. This is mainly because the noise components across adjacent frequency bins are strongly correlated in this example, and thus the cross-covariance tensors used in DC-CPD are rather noisy. This also explains the relatively poor performance of CPD-C. For GOJD, we have observed that it generates good performance at high SNR, while relatively poor performance at low SNR. The good performance of GOJD at high SNR is mainly the result of prewhitening.

In Fig. 5 (b) we note that SOBIUM and CPD-C do not provide the correct result in this highly underdetermined setting. On the other hand, DC-CPD-ALG, DC-CPD-ALS and DC-CPD-SDF still perform quite well. DC-CPD-ALS and DC-CPD-SDF perform better than DC-CPD-ALG. Comparing the two sub-figures in Fig. 5, there is more improvement by optimization based algorithms over DC-CPD-ALG, in this difficult highly underdetermined case, than in the overdetermined case.

## V. CONCLUSION

In this study, we have considered the problem of DC-CPD for J-BSS of multi-set signals. We have shown how, via the use of second-order statistics, a DC-CPD problem can be obtained from the multi-set signals in J-BSS. We have proposed an algebraic DC-CPD algorithm, via the use of the coupled rank-1 detection mapping, which is of particular interest in underdetermined problems. Deterministic and generic uniqueness conditions of DC-CPD have been studied, and shown to be more relaxed than their CPD equivalents. The proposed algorithm is deterministic and returns the exact solution in the noiseless case, as long as the uniqueness condition is satisfied. When noise is present, the proposed algorithm can serve to provide a low-cost initialization for optimization based algo-

gorithms. Experiments are performed to compare DC-CPD and CPD based BSS methods, with particular emphasis on underdetermined J-BSS problems. We also provide results of overdetermined J-BSS experiments, in comparison with existing J-BSS algorithms. The results have generally shown the superiority of using DC-CPD for J-BSS, with respect to uniqueness and accuracy.

## APPENDIX I PROOFS

*Theorem 1:*

Assuming that  $\mathbf{X}^{(1)}, \dots, \mathbf{X}^{(K)}$  are nonzero matrices, we have, by definition, that  $\text{vec}(\Phi_{(k_1, k_2)}(\mathbf{X}^{(1)}, \dots, \mathbf{X}^{(K)}))$  in (13) is an all-zero vector if and only if  $\mathbf{X}^{(k_1)}$  and  $\mathbf{X}^{(k_2)}$  are both rank-1 and have identical column spaces. Then *Theorem 1* holds as  $\Psi(\mathbf{X}^{(1)}, \dots, \mathbf{X}^{(K)})$  is defined as the concatenation of  $\text{vec}(\Phi_{(k_1, k_2)}(\mathbf{X}^{(1)}, \dots, \mathbf{X}^{(K)}))$  for all possible values of  $(k_1, k_2)$ . ■

*Theorem 4:*

We prove the following partial statements:

(i)  $\ker(\mathbf{\Gamma}^{(m, n_1, \dots, n_K)}) = \ker((\mathbf{P}_{n_1, \dots, n_K}^{(m)})^T)$ .

(ii)  $\dim(\mathbf{\Gamma}^{(m, n_1, \dots, n_K)}) = R$ .

(iii) The basis vectors  $\mathbf{w}_r^{(m, n_1, \dots, n_K)}$  in  $\ker(\mathbf{\Gamma}^{(m, n_1, \dots, n_K)})$ ,  $r = 1, \dots, R$ , can be written as a linear combination of vectors  $\mathbf{b}_u^{(m, n_1)} \otimes \dots \otimes \mathbf{b}_u^{(m, n_K)}$ ,  $u = 1, \dots, R$ , where  $[\mathbf{b}_1^{(m, n_k)}, \dots, \mathbf{b}_R^{(m, n_k)}] = \mathbf{B}^{(m, n_k)} \triangleq (\mathbf{C}^{(m, n_k)} \mathbf{D}^{(m, n_k)} \mathbf{\Pi})^T \in \mathbb{C}^{R \times R}$ ,  $\mathbf{D}^{(m, n_k)}$  is a diagonal matrix, and  $\mathbf{\Pi}$  is a permutation matrix that is common to all the matrices  $\mathbf{B}^{(m, n_k)}$ ,  $k = 1, \dots, K$ .

Note that  $m, n_1, \dots, n_K$  are fixed in the above statements.

First, as  $\Phi_{n_1, \dots, n_K}^{(m)}$  is assumed to have full column rank, and  $\mathbf{\Gamma}^{(m, n_1, \dots, n_K)} = \Phi_{n_1, \dots, n_K}^{(m)} (\mathbf{P}_{n_1, \dots, n_K}^{(m)})^T$ , we have  $\ker(\mathbf{\Gamma}^{(m, n_1, \dots, n_K)}) = \ker((\mathbf{P}_{n_1, \dots, n_K}^{(m)})^T)$ .

Second, as  $\mathbf{C}^{(m, n_1)}, \dots, \mathbf{C}^{(m, n_K)}$  have full column rank, the Kronecker product  $\mathbf{C}^{(m, n_1)} \otimes \dots \otimes \mathbf{C}^{(m, n_K)}$  also has full column rank. The  $R^K \times (R^K - R)$  matrix  $\mathbf{P}_{n_1, \dots, n_K}^{(m)}$  has full column rank as well, since its columns constitute a subset of the columns of  $\mathbf{C}^{(m, n_1)} \otimes \dots \otimes \mathbf{C}^{(m, n_K)}$ . By the rank nullity theorem, which states that  $\dim[\ker(\mathbf{A})] + \text{rank}(\mathbf{A}) = J$  for any matrix  $\mathbf{A}$  of size  $I \times J$ , we have:

$$\dim[\ker((\mathbf{P}_{n_1, \dots, n_K}^{(m)})^T)] = R^K - \text{rank}((\mathbf{P}_{n_1, \dots, n_K}^{(m)})^T) = R.$$

Third, we prove that  $\mathbf{b}_r^{(m, n_1)} \otimes \dots \otimes \mathbf{b}_r^{(m, n_K)}$  is in  $\ker((\mathbf{P}_{n_1, \dots, n_K}^{(m)})^T)$ ,  $r = 1, \dots, R$ . This is equivalent to proving the following for all the values  $1 \leq r_1, \dots, r_K \leq R$ :

$$\begin{aligned} & (\mathbf{c}_{r_1}^{(m, n_1)} \otimes \dots \otimes \mathbf{c}_{r_K}^{(m, n_K)})^T (\mathbf{b}_r^{(m, n_1)} \otimes \dots \otimes \mathbf{b}_r^{(m, n_K)}) \\ &= (\mathbf{c}_{r_1}^{(m, n_1)T} \mathbf{b}_r^{(m, n_1)}) \otimes \dots \otimes (\mathbf{c}_{r_K}^{(m, n_K)T} \mathbf{b}_r^{(m, n_K)}) = 0. \end{aligned} \quad (38)$$

Recall that  $\mathbf{b}_r^{(m, n_k)}$  is the  $r$ th column of  $(\tilde{\mathbf{C}}^{(m, n_k)})^{-T}$ , where  $\tilde{\mathbf{C}}^{(m, n_k)} = \mathbf{C}^{(m, n_k)} \mathbf{D}^{(m, n_k)} \mathbf{\Pi}$ . We assume the matrix  $\mathbf{\Pi}$  permutes the columns of  $\mathbf{C}^{(m, n_k)}$  in such a way that  $(\mathbf{C}^{(m, n_k)} \mathbf{\Pi})_{:,r} = \mathbf{c}_u^{(m, n_k)}$ , where  $r = \pi(u)$ ,  $1 \leq u \leq R$ , and  $(\pi(1), \dots, \pi(R))$  is a permutation of  $(1, \dots, R)$ . We denote  $\tilde{\mathbf{c}}_r^{(m, n_k)}$  as the  $r$ th column of  $\tilde{\mathbf{C}}^{(m, n_k)}$ . By definition we have  $\tilde{\mathbf{c}}_r^{(m, n_k)} = d_r^{(m, n_k)} \mathbf{c}_u^{(m, n_k)}$ , where  $d_r^{(m, n_k)}$  is the  $r$ th entry on the diagonal of  $\mathbf{D}^{(m, n_k)}$ .

Therefore, we have  $\mathbf{c}_k^{(m,n_k)T} \mathbf{b}_r^{(m,n_k)} = 0$  if  $r = \pi(u)$  and  $u \neq r_k$ . Since at least two of the indices  $r_1, \dots, r_K$  are distinct according to the definition of  $\mathbf{P}_{m, \dots, n_K}^{(m)}$ , at least one term in  $\mathbf{c}_r^{(m,n_1)T} \mathbf{b}_r^{(m,n_1)}, \dots, \mathbf{c}_r^{(m,n_K)T} \mathbf{b}_r^{(m,n_K)}$  is equal to zero, which proves (38). Moreover, as  $\mathbf{b}_1^{(m,n_k)}, \dots, \mathbf{b}_R^{(m,n_k)}$  are linearly independent, the set  $\{\mathbf{b}_r^{(m,n_1)} \otimes \dots \otimes \mathbf{b}_r^{(m,n_K)}, r = 1, \dots, R\}$  contains  $R$  linearly independent vectors, and thus is a maximal set of linearly independent vectors of  $\ker(\mathbf{\Gamma}^{(m,n_1, \dots, n_K)})$ . Therefore, the basis vectors  $\mathbf{w}_r^{(m,n_1, \dots, n_K)}$  of  $\ker(\mathbf{\Gamma}^{(m,n_1, \dots, n_K)})$  can be expressed as a linear combination of  $\mathbf{b}_r^{(m,n_1)} \otimes \dots \otimes \mathbf{b}_r^{(m,n_K)}$ ,  $r = 1, \dots, R$ . ■

ACKNOWLEDGMENT

The authors would like to express their sincere gratitude to Dr. Ignat Domanov and Dr. Mikael Sorensen for their insightful comments on the algebraic DC-CPD algorithm.

REFERENCES

[1] N. D. Sidiropoulos, G. Giannakis, R. Bro, "Blind PARAFAC receivers for DS-CDMA systems," *IEEE Trans. Signal Process.*, vol. 48, no. 3, pp. 810–823, Mar. 2000.

[2] N. D. Sidiropoulos, R. Bro, G. B. Giannakis, "Parallel factor analysis in sensor array processing," *IEEE Trans. Signal Process.*, vol. 48, no. 8, pp. 2377–2388, Aug. 2000.

[3] M. Mørup, "Applications of tensor (multiway array) factorizations and decompositions in data mining," *Wiley Interdisciplinary Reviews: Data Mining and Knowledge Discovery*, vol. 1, no. 1, pp. 24–40, Jan. 2011.

[4] F.-Y. Cong, Q.-H. Lin, L.-D. Kuang, X.-F. Gong, P. Astikainen, T. Ristaniemi, "Tensor decomposition of EEG signals: a brief review," *J. Neurosci. Meth.*, vol. 248, pp. 59–69, Jun. 2015.

[5] A. Cichocki, D. Mandic, A.-H. Phan, C. Caiafa, G.-X. Zhou, Q.-B. Zhao, L. De Lathauwer, "Tensor decompositions for signal processing applications. From two-way to multiway component analysis," *IEEE Signal Process. Mag.*, vol. 32, no. 2, pp. 145–163, Mar. 2015.

[6] P. Comon, L. De Lathauwer, "Algebraic identification of underdetermined mixtures," in *Handbook of blind source separation, independent component analysis and applications*. P. Comon, and C. Jutten, ed., U.K.: Academic Press, 2010, pp. 325–365.

[7] T. Kolda, B. Bader, "Tensor decompositions and applications," *SIAM Review*, vol. 51, no. 3, pp. 455–500, Sep. 2009.

[8] N. D. Sidiropoulos, L. De Lathauwer, X. Fu, K. Huang, E. E. Papalexakis, C. Faloutsos, "Tensor decomposition for signal processing and machine learning," arXiv: 1607.01668v1. 2016.

[9] R. Harshman, M. Lundy, "PARAFAC: Parallel factor analysis," *Comput. Stat. Data Anal.*, vol. 18, no. 1, pp. 39–72, Aug. 1994.

[10] L. De Lathauwer, "A link between the canonical decomposition in multilinear algebra and simultaneous matrix diagonalization," *SIAM J. Matrix Anal. Appl.*, vol. 28, no. 3, pp. 642–666, Sep. 2006.

[11] L. De Lathauwer, J. Castaing, "Blind identification of underdetermined mixtures by simultaneous matrix diagonalization," *IEEE Trans. Signal Process.*, vol. 56, no. 3, pp. 1096–1105, Mar. 2008.

[12] I. Domanov, L. De Lathauwer, "Canonical polyadic decomposition of third-order tensors: reduction to generalized eigenvalue decomposition," *SIAM J. Matrix Anal. Appl.*, vol. 35, no. 2, pp. 636–660, May 2014.

[13] I. Domanov, L. De Lathauwer, "Canonical polyadic decomposition of third-order tensors: relaxed uniqueness conditions and algebraic algorithm," *Linear Algebra Appl.*, vol. 513, pp. 342–375, Jan. 2017.

[14] L. Sorber, M. Van Barel, L. De Lathauwer, "Optimization-based algorithms for tensor decompositions: canonical polyadic decomposition, decomposition in rank- $(L_r, L_r, 1)$  terms, and a new generalization," *SIAM J. Matrix Anal. Appl.*, vol. 23, no. 2, pp. 695–720, Apr. 2013.

[15] P. Paatero, "The multilinear engine—a table-driven, least squares program for solving multilinear problems, including the n-way

parallel factor analysis model," *J. Comput. Graph. Stat.*, vol. 8, no. 4, pp. 854–888, Dec. 1999.

[16] A.-H. Phan, P. Tichavsky, A. Cichocki, "Low complexity damped Gauss-Newton algorithms for CANDECOMP/PARAFAC," *SIAM J. Matrix Anal. Appl.*, vol. 34, no. 1, pp. 126–147, Jan. 2013.

[17] J. B. Kruskal, "Three-way arrays: Rank and uniqueness of trilinear decompositions, with applications to arithmetic complexity and statistics," *Linear Algebra Appl.*, vol. 18, no. 2, pp. 95–138, Dec. 1977.

[18] L. Chiantini, G. Ottaviani, "On generic identifiability of 3-tensors of small rank," *SIAM J. Matrix Anal. Appl.*, vol. 33, no. 3, pp. 1018–1037, Jul. 2012.

[19] I. Domanov, L. De Lathauwer, "On the uniqueness of the canonical polyadic decomposition of third-order tensors—Part I: basic results and uniqueness of one factor matrix," *SIAM J. Matrix Anal. Appl.*, vol. 34, no. 3, pp. 855–875, Jul. 2013.

[20] I. Domanov, L. De Lathauwer, "On the uniqueness of the canonical polyadic decomposition of third-order tensors—Part II: uniqueness of the overall decomposition," *SIAM J. Matrix Anal. Appl.*, vol. 34, no. 3, pp. 876–903, Jul. 2013.

[21] I. Domanov, L. De Lathauwer, "Generic uniqueness conditions for the canonical polyadic decomposition and INDSCAL," *SIAM J. Matrix Anal. Appl.*, vol. 36, no. 4, pp. 1567–1589, Nov. 2015.

[22] M. Sorensen, L. De Lathauwer, "New uniqueness conditions for the canonical polyadic decomposition of third-order tensors," *SIAM J. Matrix Anal. Appl.*, vol. 36, no. 4, pp. 1381–1403, Oct. 2015.

[23] A. Cichocki, R. Zdunek, A.-H. Phan, S. Amari, "Multi-way array (tensor) factorizations and decompositions," in *Nonnegative matrix and tensor factorizations: Applications to exploratory multi-way data analysis and blind source separation*. Singapore: John Wiley & Sons, 2009, pp. 337–432.

[24] G.-X. Zhou, A. Cichocki, "Canonical polyadic decomposition based on a single mode blind source separation," *IEEE Signal Process. Lett.*, vol. 19, no. 8, pp. 523–526, Aug. 2012.

[25] M. De Vos, D. Nion, S. Van Huffel, L. De Lathauwer, "A combination of parallel factor and independent component analysis," *Signal Process.*, vol. 92, no. 12, pp. 2990–2999, Dec. 2012.

[26] M. Sorensen, L. De Lathauwer, "Blind signal separation via tensor decomposition with Vandermonde factor: Canonical polyadic decomposition," *IEEE Trans. Signal Process.*, vol. 61, no. 22, pp. 5507–5519, Nov. 2012.

[27] L. De Lathauwer, J. Castaing, "Tensor-based techniques for the blind separation of DS-CDMA signals," *Signal Process.*, vol. 87, no. 2, pp. 322–336, Feb. 2007.

[28] M. Sorensen, L. De Lathauwer, P. Comon, S. Icart, L. Deneire, "Canonical polyadic decomposition with a columnwise orthonormal factor matrix," *SIAM J. Matrix Anal. Appl.*, vol. 33, no. 4, pp. 1190–1213, Oct. 2012.

[29] J. Sui, T. Adali, Q.-B. Yu, V. Calhoun, "A Review of multivariate methods for multimodal fusion of brain imaging data," *J. Neurosci. Meth.*, vol. 204, pp. 68–81, Feb. 2012.

[30] T. Kim, H. T. Attias, S.-Y. Lee, T.-W. Lee, "Blind source separation exploiting higher-order frequency dependencies," *IEEE Trans. Audio, Speech, Lang. Process.*, vol. 15, no. 1, pp. 70–79, Jan. 2007.

[31] J.-H. Lee, T.-W. Lee, F. Jolesz, S.-S. Yoo, "Independent vector analysis (IVA): multivariate approach for fMRI group study," *NeuroImage*, vol. 40, no. 1, pp. 86–109, Mar. 2008.

[32] M. Anderson, T. Adali, and X.-L. Li, "Joint blind source separation with multivariate Gaussian model: algorithms and performance analysis," *IEEE Trans. Signal Process.*, vol. 60, no. 4, pp. 1672–1683, Apr. 2012.

[33] Y.-O. Li, T. Adali, W. Wang, V. Calhoun, "Joint blind source separation by multiset canonical correlation analysis," *IEEE Trans. Signal Process.*, vol. 57, no. 10, pp. 3918–3929, Oct. 2009.

[34] N. M. Correa, T. Eichele, T. Adali, Y.-O. Li, V. D. Calhoun, "Multi-set canonical correlation analysis for the fusion of concurrent single trial ERP and functional MRI," *NeuroImage*, vol. 50, no. 4, pp. 1438–1445, May 2010.

- [35] N. M. Correa, T. Adali, V. D. Calhoun, "Canonical correlation analysis for data fusion and group analysis: Examining applications of medical imaging data," *IEEE Signal Process. Mag.*, vol. 27, no. 4, pp. 39–50, Jul. 2010.
- [36] J. Chatel-Goldman, M. Congedo, R. Phlypo, "Joint BSS as a natural analysis framework for EEG-hyperscanning," in *Proc. ICASSP'2013*, Vancouver, Canada, May 26–30, 2013.
- [37] X.-L. Li, T. Adali, M. Anderson, "Joint blind source separation by generalized joint diagonalization of cumulant matrices," *Signal Process.*, vol. 91, no. 10, pp. 2314–2322, Oct. 2011.
- [38] M. Congedo, R. Phlypo, J. Chatel-Goldman, "Orthogonal and non-orthogonal joint blind source separation in the least-squares sense," in *Proc. EUSIPCO'2012*, Bucharest, Romania, Aug. 27–31, 2012.
- [39] X.-F. Gong, X.-L. Wang, Q.-H. Lin, "Generalized non-orthogonal joint diagonalization with LU decomposition and successive rotations," *IEEE Trans. Signal Process.*, vol. 63, no. 5, pp. 1322–1334, Mar. 2015.
- [40] D. Lahat, T. Adali, C. Jutten, "Multimodal data fusion: an overview of methods, challenges, and prospects," *Proc. IEEE*, vol. 103, no. 9, pp. 1449–1477, Sep. 2015.
- [41] R. Harshman, M. Lundy. (1984b), "Data preprocessing and the extended PARAFAC model," in H. Law, C. Snyder Jr, J. Hattie, R. McDonald, ed., *Research methods for multimode data analysis*, Praeger, New York, 1984, pp. 216–284.
- [42] C. Beckmann, S. Smith, "Tensorial extensions of independent component analysis for multisubject fMRI analysis," *NeuroImage*, vol. 25, no. 1, pp. 294–311, Mar. 2005.
- [43] Y. Guo, G. Pagnoni, "A unified framework for group independent component analysis for multi-subject fMRI data," *NeuroImage*, vol. 42, no. 3, pp. 1078–1093, Sep. 2008.
- [44] A. Groves, C. Beckmann, S. Smith, M. Woolrich, "Linked independent component analysis for multimodal data fusion," *NeuroImage*, vol. 54, no. 3, pp. 2198–2217, Feb. 2011.
- [45] E. Acar, R. Bro, A. K. Smilde, "Data fusion in metabolomics using coupled matrix and tensor factorizations," *Proc. IEEE*, vol. 103, no. 9, pp. 1602–1620, Sep. 2015.
- [46] M. Sorensen, L. De Lathauwer, "Multiple invariance ESPRIT for nonuniform linear arrays: a coupled canonical polyadic decomposition approach," *IEEE Trans. Signal Process.*, vol. 64, no. 14, pp. 3693–3704, Jul. 2016.
- [47] Y.-N. Yu, A. Petropulu, "PARAFAC-based blind estimation of possibly underdetermined convolutive MIMO systems," *IEEE Trans. Signal Process.*, vol. 56, no. 1, pp. 111–124, Jan. 2008.
- [48] H. Becker, P. Comon, L. Albera, "Tensor-based preprocessing of combined EEG/MEG data," in *Proc. EUSIPCO'2012*, Bucharest, Romania, Aug. 27–31, 2012, pp. 275–279.
- [49] X.-F. Gong, Y. -N. Hao, Q. -H. Lin, "Joint canonical polyadic decomposition of two tensors with one shared loading matrix" in *Proc. MLSP'2013*, Southampton, U. K., Sep. 22–25, 2013.
- [50] T. Yokota, A. Cichocki, Y. Yamashita, "Linked PARAFAC / CP tensor decomposition and its fast implementation for multi-block tensor analysis," in *Proc. ICONIP'2012*, Doha, Qatar, Nov. 12–15, 2012, pp. 84–92.
- [51] M. Sorensen, L. De Lathauwer, "Coupled canonical polyadic decompositions and (coupled) decompositions in multilinear rank- $(L_{r,n}, L_{r,n}, 1)$  terms—Part I: uniqueness," *SIAM J. Matrix Anal. Appl.*, vol. 36, no. 2, pp. 496–522, May 2015.
- [52] M. Sorensen, I. Domanov, L. De Lathauwer, "Coupled canonical polyadic decompositions and (coupled) decompositions in multilinear rank- $(L_{r,n}, L_{r,n}, 1)$  terms—Part II: algorithms," *SIAM J. Matrix Anal. Appl.*, vol. 36, no. 3, pp. 1015–1045, Jul. 2015.
- [53] M. Sorensen, L. De Lathauwer, "Multidimensional harmonic retrieval via coupled canonical polyadic decompositions—Part I: model and identifiability," *IEEE Trans. Signal Process.*, vol. 65, no. 2, pp. 517–527, Jan. 2017.
- [54] M. Sorensen, L. De Lathauwer, "Multidimensional harmonic retrieval via coupled canonical polyadic decompositions—Part II: algorithm and multirate sampling," *IEEE Trans. Signal Process.*, vol. 65, no. 2, pp. 528–539, Jan. 2017.
- [55] M. Sorensen, L. De Lathauwer, "Coupled tensor decompositions in array processing," ESAT-STADIUS, KU Leuven, Belgium, Tech. Rep. 13–241, 2014.
- [56] R. Farias, J. Cohen, P. Comon, "Exploring multimodal data fusion through joint decompositions with flexible couplings," *IEEE Trans. Signal Process.*, vol. 64, no. 18, pp. 4830–4844, Sept. 2016.
- [57] B. Rivet, M. Duda, A. Guérin-Dugué, C. Jutten, P. Comon, "Multimodal approach to estimate the ocular movements during EEG recordings: a coupled tensor factorization method," in *Proc. EMBC'2015*, Milan, Italy, Aug. 25–29, 2015.
- [58] G.-X. Zhou, Q.-B. Zhao, Y. Zhang, T. Adali, S.-L. Xie, A. Cichocki, "Linked component analysis from matrices to high order tensors: applications to biomedical data," *Proc. IEEE*, vol. 104, no. 2, pp. 310–331, Feb. 2016.
- [59] M. Sorensen, L. De Lathauwer, "Double coupled canonical polyadic decomposition with applications," ESAT-STADIUS, KU Leuven, Belgium, Tech. Rep. 13–145, 2013.
- [60] O. Debals, L. De Lathauwer, "Stochastic and deterministic tensorization for blind signal separation," in *Proc. LVA/ICA'2015*, Liberec, Czech Republic, Aug. 25–28, 2015, pp. 3–13.
- [61] E. Sanchez, L. S. Ramos, B. R. Kowalski, "Generalized rank annihilation method : I. Application to liquid chromatography—diode array ultraviolet detection data," *J. Chromatogr. A*, vol. 385, no. 1, pp. 151–164, Jan. 1987.
- [62] L. Wang, H. Ding, F. -L. Yin, "A region-growing permutation alignment approach in frequency-domain blind source separation of speech mixtures," *IEEE Trans. Audio, Speech, Lang. Process.*, vol. 19, no. 3, pp. 549–557, Mar. 2011.
- [63] L. Sorber, M. Van Barel, L. De Lathauwer, "Structured data fusion," *IEEE J. Sel. Topics Signal Process.*, vol. 9, no. 4, pp. 586–600, Jun. 2015.
- [64] N. Vervliet, O. Debals, L. Sorber, M. Van Barel, and L. De Lathauwer, *Tensorlab 3.0*, Mar. 2016. [Online], Available: <http://www.tensorlab.net/>.
- [65] R. Gunning, H. Rossi, "Holomorphic functions" in *Analytic functions of several complex variables*. U.S.: Prentice-Hall, Inc, Englewood Cliffs, N.J., 1965, pp. 1–63.
- [66] G. Golub, C. Van Loan, "Orthogonalization and least squares," in *Matrix computations, fourth edition*. G. Golub, C. Van Loan, ed., U.S.A: The Johns Hopkins University Press, 2013, pp. 233–298.
- [67] E. Vincent, Evaluation and audio source separation software [Online], Available: <http://www.irisa.fr/metiss/members/evincent/softwareA>.
- [68] Q. Shen, W. Liu, W. Cui, S. -L. Wu, Y. -M. Zhang, M. Amin, "Low-complexity direction-of-arrival estimation based on wideband co-prime arrays," *IEEE/ACM Trans. Audio, Speech, Language Process.*, vol. 23, no. 9, pp. 1445–1456, Sep. 2015.



# Double Coupled Canonical Polyadic Decomposition for Joint Blind Source Separation

Xiao-Feng Gong, *Member, IEEE*, Qiu-Hua Lin, *Member, IEEE*, Feng-Yu Cong, *Senior Member, IEEE*, and Lieven De Lathauwer, *Fellow, IEEE*

## Supplementary materials

### I. DERIVATION OF ALGEBRAIC DC-CPD ALGORITHM IN THE GENERAL CASE

We explain (i) the derivation of equation (22), and (ii) the computation of the  $(K+1)$ th-order overdetermined C-CPD (24).

#### A. Derivation of equation (22)

Recall that the  $\mathbb{C}_K^2 N^{2K} \times R^K$  matrix  $\mathbf{\Gamma}^{(m, n_1, \dots, n_K)}$  is the matricized version of  $(K+1)$ th-order tensor  $\mathcal{G}^{(m, n_1, \dots, n_K)}$ :

$$\left[ \mathbf{\Gamma}^{(m, n_1, \dots, n_K)} \right]_{(l, :)} \triangleq \text{vec} \left( \left[ \mathcal{G}^{(m, n_1, \dots, n_K)} \right]_{(l, :, \dots, :)} \right)^T, \quad (\text{S1})$$

where  $\mathcal{G}^{(m, n_1, \dots, n_K)}$  is defined as:

$$\left[ \mathcal{G}^{(m, n_1, \dots, n_K)} \right]_{(:, r_1, \dots, r_K)} \triangleq \psi \left( \mathcal{T}_{(:, :, r_1)}^{(m, n_1)}, \dots, \mathcal{T}_{(:, :, r_K)}^{(m, n_K)} \right). \quad (\text{S2})$$

The operation  $\psi(\cdot)$  is defined in (10) as:

$$\psi \left( \mathbf{X}^{(1)}, \dots, \mathbf{X}^{(K)} \right) \triangleq \begin{bmatrix} \text{vec} \left( \Phi_{(1,2)} \left( \mathbf{X}^{(1)}, \dots, \mathbf{X}^{(K)} \right) \right) \\ \text{vec} \left( \Phi_{(1,3)} \left( \mathbf{X}^{(1)}, \dots, \mathbf{X}^{(K)} \right) \right) \\ \vdots \\ \text{vec} \left( \Phi_{(K-1,K)} \left( \mathbf{X}^{(1)}, \dots, \mathbf{X}^{(K)} \right) \right) \end{bmatrix}, \quad (\text{S3})$$

where  $\Phi_{(k_1, k_2)}(\cdot)$  is the  $K$ th-order coupled rank-1 detection mapping,  $1 \leq k_1 < k_2 \leq K$ , defined in (9) as:

$$\left[ \Phi_{(k_1, k_2)} \left( \mathbf{X}^{(1)}, \dots, \mathbf{X}^{(K)} \right) \right]_{i_1 \dots i_{k_1}, j_1 \dots j_{k_2}} \triangleq \begin{vmatrix} \mathbf{x}_{i_{k_1}, j_{k_1}}^{(k_1)} & \mathbf{x}_{i_{k_1}, j_{k_2}}^{(k_2)} \\ \mathbf{x}_{i_{k_2}, j_{k_1}}^{(k_1)} & \mathbf{x}_{i_{k_2}, j_{k_2}}^{(k_2)} \end{vmatrix} \prod_{l \in \{k_1, k_2\}} \mathbf{x}_{i_l, j_l}^{(l)}. \quad (\text{S4})$$

Due to the multilinearity of  $\psi$ , we have:

$$\mathbf{\Gamma}^{(m, n_1, \dots, n_K)} = \sum_{r_1, \dots, r_K=1}^R \left[ \psi \left( \mathbf{a}_{r_1}^{(m)} \mathbf{a}_{r_1}^{(n_1)H}, \dots, \mathbf{a}_{r_K}^{(m)} \mathbf{a}_{r_K}^{(n_K)H} \right) \cdot \left( \mathbf{e}_{r_1}^{(m, n_1)} \otimes \dots \otimes \mathbf{e}_{r_K}^{(m, n_K)} \right)^T \right]. \quad (\text{S5})$$

According to *Theorem 1*,  $\psi \left( \mathbf{a}_{r_1}^{(m)} \mathbf{a}_{r_1}^{(n_1)H}, \dots, \mathbf{a}_{r_K}^{(m)} \mathbf{a}_{r_K}^{(n_K)H} \right) = \mathbf{0}$  when  $r_1 = \dots = r_K$  and thus (S5) can be rewritten as:

$$\mathbf{\Gamma}^{(m, n_1, \dots, n_K)} = \sum_{(r_1, \dots, r_K) \in \Theta^{(K)}} \left[ \psi \left( \mathbf{a}_{r_1}^{(m)} \mathbf{a}_{r_1}^{(n_1)H}, \dots, \mathbf{a}_{r_K}^{(m)} \mathbf{a}_{r_K}^{(n_K)H} \right) \cdot \left( \mathbf{e}_{r_1}^{(m, n_1)} \otimes \dots \otimes \mathbf{e}_{r_K}^{(m, n_K)} \right)^T \right], \quad (\text{S6})$$

where  $\Theta^{(K)}$  is the set of tuples  $(r_1, \dots, r_K)$ ,  $1 \leq r_1 \leq \dots \leq r_K \leq R$ , in which each tuple contains at least two distinct elements. We stack the vectors  $\mathbf{e}_{r_1}^{(m, n_1)} \otimes \dots \otimes \mathbf{e}_{r_K}^{(m, n_K)}$  into a  $R^K \times (R^K - R)$

matrix  $\mathbf{P}^{(m)}$ , and the vectors  $\psi \left( \mathbf{a}_{r_1}^{(m)} \mathbf{a}_{r_1}^{(n_1)H}, \dots, \mathbf{a}_{r_K}^{(m)} \mathbf{a}_{r_K}^{(n_K)H} \right)$  into a  $\mathbb{C}_K^2 N^{2K} \times (R^K - R)$  matrix  $\mathbf{\Phi}^{(m)}$ , where these vectors are indexed by tuples  $(r_1, \dots, r_K) \in \Theta^{(K)}$ . Then (S6) can be rewritten as  $\mathbf{\Gamma}^{(m, n_1, \dots, n_K)} = \mathbf{\Phi}^{(m)} \left( \mathbf{P}_{n_1, \dots, n_K}^{(m)} \right)^T$  (equation (22) in the paper).

#### B. Computation of overdetermined C-CPD (24)

We copy (24) here:

$$\mathcal{W}^{(m, n_1, \dots, n_K)} = \left[ \mathbf{B}^{(m, n_1)}, \dots, \mathbf{B}^{(m, n_K)}, \mathbf{F}^{(m, n_1, \dots, n_K)} \right]_R, \quad (\text{S7})$$

where  $\mathbf{B}^{(m, n_k)} = \tilde{\mathbf{C}}^{(m, n_k)T} \in \mathbb{C}^{R \times R}$ ,  $\tilde{\mathbf{C}}^{(m, n_k)} \triangleq \mathbf{C}^{(m, n_k)} \mathbf{D}_C^{(m, n)} \mathbf{\Pi}$ ,  $\mathbf{D}_C^{(m, n)}$  is a diagonal matrix, and  $\mathbf{\Pi}$  is a common permutation matrix for all  $\mathbf{B}^{(m, n_k)}$ ,  $k = 1, \dots, K$ . For all the possible values of  $1 \leq m \leq M$  and  $1 \leq n_1 < \dots < n_K \leq M$ , (S7) is a  $(K+1)$ th-order overdetermined C-CPD with coupling in the first  $K$  modes.

When  $K = 2$ , (S7) is an overdetermined DC-CPD and we can use the strategy explained in Subsection III.D. for its computation. When  $K > 2$ , the tensor  $\mathcal{W}^{(m, n_1, \dots, n_K)}$  in (S7) has order  $(K+1) > 3$ . We now follow [1], in which it is explained that, under conditions that are satisfied in our derivation, the CPD of a tensor of order higher than three can equivalently be expressed as a C-CPD of third-order tensors obtained by combining modes. Briefly, for each tensor  $\mathcal{W}^{(m, n_1, \dots, n_K)}$  in (S7), we consider:

$$\mathcal{V}_w^{(m, n_1, \dots, n_K)} = \left[ \mathbf{B}_w^{(m, n_1, \dots, n_K)}, \mathbf{B}_w^{(m, n_1, \dots, n_K)}, \mathbf{F}^{(m, n_1, \dots, n_K)} \right]_R, \quad (\text{S8})$$

where:

$$\begin{cases} \mathbf{B}_w^{(m, n_1, \dots, n_K)} \triangleq \odot_{u \in \Omega_w^{(m, n_1, \dots, n_K)}} \mathbf{B}^{(m, u)} \in \mathbb{C}^{\text{card}(\Omega_w^{(m, n_1, \dots, n_K)}) \times R \times R} \\ \mathbf{B}_w^{(m, n_1, \dots, n_K)} \triangleq \odot_{v \in \Omega_w^{(m, n_1, \dots, n_K)}} \mathbf{B}^{(m, v)} \in \mathbb{C}^{\text{card}(\Omega_w^{(m, n_1, \dots, n_K)}) \times R \times R} \\ \Omega_w^{(m, n_1, \dots, n_K)} \cup \Omega_w^{(m, n_1, \dots, n_K)} = \{n_1, \dots, n_K\} \\ \Omega_w^{(m, n_1, \dots, n_K)} \cap \Omega_w^{(m, n_1, \dots, n_K)} = \emptyset, \end{cases}$$

where  $\Omega_w^{(m, n_1, \dots, n_K)}$  and  $\Omega_w^{(m, n_1, \dots, n_K)}$  are two complementary sets of numbers taken from  $\{n_1, \dots, n_K\}$ ,  $w = 1, \dots, W^{(m, n_1, \dots, n_K)}$ , and  $W^{(m, n_1, \dots, n_K)}$  is the number of all the possible sets  $\Omega_w^{(m, n_1, \dots, n_K)}$  (or  $\Omega_w^{(m, n_1, \dots, n_K)}$ ) for fixed  $(m, n_1, \dots, n_K)$ ,  $1 \leq n_1 < \dots < n_K \leq M$ ,  $m = 1, \dots, M$ . The above operations combine the modes, whose indices belong to the set  $\Omega_w^{(m, n_1, \dots, n_K)}$ , into the first mode of  $\mathcal{V}_w^{(m, n_1, \dots, n_K)}$ , and combine the remaining modes into the second mode of  $\mathcal{V}_w^{(m, n_1, \dots, n_K)}$ . All the tensors  $\mathcal{V}_w^{(m, n_1, \dots, n_K)}$  with fixed  $(m, n_1, \dots, n_K)$  and different  $w$  are coupled in the third mode,

and this C-CPD can be computed by a GEVD, as explained in [1]. Therefore, any of the  $(K+1)$ th-order CPDs can be computed by GEVD, which yields us the factor matrices  $\mathbf{B}^{(m,n_1)}, \dots, \mathbf{B}^{(m,n_K)}$ , for any choice of  $(m, n_1, \dots, n_K)$ . Then we work in analogy with (17) and (18) to obtain all the factor matrices  $\mathbf{B}^{(m,n)}$ ,  $m, n = 1, \dots, M$ . More precisely, assume for instance that  $\mathbf{B}^{(m,1)}$  has been found, then for tensor  $\mathcal{W}^{(m,1,n_2,\dots,n_K)}$ , we have:

$$\mathbf{W}_1^{(m,1,n_2,\dots,n_K)} \mathbf{B}^{(m,1)-T} = \mathbf{B}^{(m,n_2)} \odot \dots \odot \mathbf{B}^{(m,n_K)} \odot \mathbf{F}^{(m,1,n_2,\dots,n_K)}. \quad (\text{S9})$$

We denote the  $r$ th column of  $\mathbf{W}_1^{(m,1,n_2,\dots,n_K)} \mathbf{B}^{(m,1)-T}$  by  $\mathbf{q}_{1,r}^{(m,1,n_2,\dots,n_K)} \in \mathbb{C}^{R^K}$  and reshape it into a tensor  $\mathcal{Q}_{1,r}^{(m,1,n_2,\dots,n_K)} = \text{Ten}(\mathbf{q}_{1,r}^{(m,1,n_2,\dots,n_K)}, [R, \dots, R]) \in \mathbb{C}^{R^K \times \dots \times R}$ . From (S9) we know that  $\mathcal{Q}_{1,r}^{(m,1,n_2,\dots,n_K)}$  is a  $K$ th-order rank-1 tensor:

$$\mathcal{Q}_{1,r}^{(m,1,n_2,\dots,n_K)} = \mathbf{b}_r^{(m,n_2)} \otimes \dots \otimes \mathbf{b}_r^{(m,n_K)} \otimes \mathbf{f}_r^{(m,n_1,\dots,n_K)}, \quad (\text{S10})$$

where  $\mathbf{b}_r^{(m,n_u)}$  and  $\mathbf{f}_r^{(m,n_1,\dots,n_K)}$  are the  $r$ th column of  $\mathbf{B}^{(m,n_u)}$  and  $\mathbf{F}^{(m,1,n_2,\dots,n_K)}$ , respectively. In the noisy case,  $\mathbf{b}_r^{(m,n_u)}$  and  $\mathbf{f}_r^{(m,n_1,\dots,n_K)}$  can be obtained by calculating the best rank-1 approximation of  $\mathcal{Q}_{1,r}^{(m,1,n_2,\dots,n_K)}$ ,  $u = 2, \dots, K$  [2]. Continuing this way, all factor matrices  $\mathbf{B}^{(m,n)}$  can be determined,  $m, n = 1, \dots, M$ .

## II. DC-CPD BY ALTERNATING LEAST SQUARES

This algorithm computes a DC-CPD by minimizing the following cost function using alternating least squares (ALS):

$$\eta = \sum_{m \leq n} \left\| \mathcal{T}^{(m,n)} - \llbracket \mathbf{A}^{(m)}, \mathbf{A}^{(n)*}, \mathbf{C}^{(m,n)} \rrbracket_R \right\|_F^2. \quad (\text{S11})$$

The idea is to update each unknown factor in the LS sense with the other factor matrices fixed and alternate over such conditional updates until convergence.

We make the following assumption, for  $1 \leq m \leq n \leq M$ , to ensure that in each ALS step, the factor matrix update is unique:

$$\begin{bmatrix} \mathbf{A}^{(1)*} \odot \mathbf{C}^{(1,m)*} \\ \vdots \\ \mathbf{A}^{(m)*} \odot \mathbf{C}^{(m,m)*} \\ \mathbf{A}^{(m+1)*} \odot \mathbf{C}^{(m,m+1)*} \\ \vdots \\ \mathbf{A}^{(M)*} \odot \mathbf{C}^{(m,M)*} \end{bmatrix} \text{ and } \mathbf{A}^{(m)} \odot \mathbf{A}^{(n)*} \text{ have full column rank.} \quad (\text{S12})$$

Equation (S12) is a necessary condition for the uniqueness of DC-CPD. In fact, if (S12) does not hold, DC-CPD with a smaller number of terms is possible. More precisely, if  $[(\mathbf{A}^{(1)*} \odot \mathbf{C}^{(1,m)*})^T, \dots, (\mathbf{A}^{(m)*} \odot \mathbf{C}^{(m,m)*})^T, (\mathbf{A}^{(m+1)*} \odot \mathbf{C}^{(m,m+1)*})^T, \dots, (\mathbf{A}^{(M)*} \odot \mathbf{C}^{(m,M)*})^T]^T$  does not have full column rank, e.g., if

$$\begin{bmatrix} \mathbf{a}_R^{(1)*} \otimes \mathbf{c}_R^{(1,m)*} \\ \vdots \\ \mathbf{a}_R^{(m)*} \otimes \mathbf{c}_R^{(m,m)*} \\ \mathbf{a}_R^{(m+1)*} \otimes \mathbf{c}_R^{(m,m+1)*} \\ \vdots \\ \mathbf{a}_R^{(M)*} \otimes \mathbf{c}_R^{(m,M)*} \end{bmatrix} = \sum_{r=1}^{R-1} \lambda_r^{(m)} \begin{bmatrix} \mathbf{a}_r^{(1)*} \otimes \mathbf{c}_r^{(1,m)*} \\ \vdots \\ \mathbf{a}_r^{(m)*} \otimes \mathbf{c}_r^{(m,m)*} \\ \mathbf{a}_r^{(m+1)*} \otimes \mathbf{c}_r^{(m,m+1)*} \\ \vdots \\ \mathbf{a}_r^{(M)*} \otimes \mathbf{c}_r^{(m,M)*} \end{bmatrix}$$

for fixed  $m$ , then  $\mathcal{T}^{(m,n)} = \sum_{r=1}^{R-1} (\mathbf{a}_r^{(m)} + \lambda_r^{(m)} \mathbf{a}_R^{(m)}) \otimes \mathbf{a}_r^{(n)*} \otimes \mathbf{c}_r^{(m,n)}$ , and  $\mathcal{T}^{(n',m)} = \sum_{r=1}^{R-1} \mathbf{a}_r^{(n')} \otimes (\mathbf{a}_r^{(m)} + \lambda_r^{(m)} \mathbf{a}_R^{(m)*}) \otimes \mathbf{c}_r^{(m,n')}$  for  $n' = 1, \dots, m$  and  $n = m, \dots, M$ . With a similar reasoning, we know that DC-CPD is possible with a smaller number of terms if  $\mathbf{A}^{(m)} \odot \mathbf{A}^{(n)*}$  does not have full column rank.

We define  $\mathcal{E}^{(m,n)} \triangleq \mathcal{T}^{(m,n)} - \llbracket \mathbf{A}^{(m)}, \mathbf{A}^{(n)*}, \mathbf{C}^{(m,n)} \rrbracket_R$  as the residue for  $\mathcal{T}^{(m,n)}$ , and  $\eta_m \triangleq \sum_{n=m}^M \|\mathcal{E}^{(m,n)}\|_F^2 + \sum_{n'=1}^m \|\mathcal{E}^{(n',m)}\|_F^2$  as the sum of LS errors for the tensors that are coupled by  $\mathbf{A}^{(m)}$ , for fixed  $m$ . Then we have  $\eta = 0.5 \cdot \sum_{m=1}^M \eta_m$ . We denote  $\mathbf{E}_1^{(m,n)}$  and  $\mathbf{E}_2^{(m,n)}$  as the mode-1 and mode-2 matrix representation of  $\mathcal{E}^{(m,n)}$ , respectively. Then  $\eta_m$  can be written as:

$$\eta_m = \sum_{n'=1}^m \|\mathbf{E}_2^{(n',m)*}\|_F^2 + \sum_{n=m}^M \|\mathbf{E}_1^{(m,n)}\|_F^2 = \left\| \begin{bmatrix} \mathbf{T}_2^{(1,m)*} \\ \vdots \\ 2\mathbf{T}_2^{(m,m)*} \\ \mathbf{T}_1^{(m,m+1)} \\ \vdots \\ \mathbf{T}_1^{(m,M)} \end{bmatrix} - \begin{bmatrix} \mathbf{A}^{(1)*} \odot \mathbf{C}^{(1,m)*} \\ \vdots \\ 2\mathbf{A}^{(m)*} \odot \mathbf{C}^{(m,m)*} \\ \mathbf{A}^{(m+1)*} \odot \mathbf{C}^{(m,m+1)*} \\ \vdots \\ \mathbf{A}^{(M)*} \odot \mathbf{C}^{(m,M)*} \end{bmatrix} \right\|_F^2. \quad (\text{S13})$$

In (S13) we have used the property that  $\mathbf{T}_1^{(m,m)} = \mathbf{T}_2^{(m,m)*}$  and  $\mathbf{C}^{(m,m)} = \mathbf{C}^{(m,m)*}$ , due to the conjugated symmetry.

We update  $\mathbf{A}^{(m)}$  by minimizing  $\eta_m$  with  $\mathbf{A}^{(1)*} \odot \mathbf{C}^{(1,m)*}, \dots, \mathbf{A}^{(m)*} \odot \mathbf{C}^{(m,m)*}, \mathbf{A}^{(m+1)*} \odot \mathbf{C}^{(m,m+1)*}, \dots, \mathbf{A}^{(M)*} \odot \mathbf{C}^{(m,M)*}$  fixed, which is an LS sub-problem that is linear in factor matrix  $\mathbf{A}^{(m)}$ .

When all the factor matrices are updated, we update  $\mathbf{C}^{(m,n)}$  for each  $(m, n)$  as follows, with  $\mathbf{A}^{(m)}$  and  $\mathbf{A}^{(n)}$  fixed:

$$\mathbf{C}^{(m,n)} = \arg \min_{\mathbf{C}^{(m,n)}} \left\| \mathbf{T}_3^{(m,n)} - (\mathbf{A}^{(m)} \odot \mathbf{A}^{(n)*}) \mathbf{C}^{(m,n)T} \right\|_F^2. \quad (\text{S14})$$

We perform the ALS steps for  $\mathbf{A}^{(m)}$  and  $\mathbf{C}^{(m,n)}$ ,  $1 \leq m \leq n \leq M$  by minimizing (S13) and (S14) in an alternating manner until convergence. To accelerate the convergence of the ALS iteration, enhanced line search (ELS) and exact line search/plane search strategies can be developed analogously to the CPD case [3]–[4]. Table I summarizes the ALS based DC-CPD algorithm.

TABLE I  
DC-CPD: ALS ALGORITHM

Input: $\{\mathcal{T}^{(m,n)} \in \mathbb{C}^{N \times N \times R}   1 \leq m, n \leq M\}$ admitting DC-CPD
1: Initialize either randomly or with the results from the algebraic DC-CPD algorithm.
2: Do the following until convergence: <ul style="list-style-type: none"> <li>- Update <math>\mathbf{A}^{(m)}</math> by minimizing (S13) with <math>\mathbf{A}^{(1)*} \odot \mathbf{C}^{(1,m)*}, \dots, \mathbf{A}^{(m)*} \odot \mathbf{C}^{(m,m)*}, \mathbf{A}^{(m+1)*} \odot \mathbf{C}^{(m,m+1)*}, \dots, \mathbf{A}^{(M)*} \odot \mathbf{C}^{(m,M)*}</math> fixed, <math>1 \leq m \leq M</math>.</li> <li>- Update <math>\mathbf{C}^{(m,n)}</math> by (S14) with <math>\mathbf{A}^{(m)}</math> and <math>\mathbf{A}^{(n)}</math> fixed, <math>1 \leq m, n \leq M</math>.</li> </ul>
Output: Estimates of the factor matrices: $\tilde{\mathbf{A}}^{(m)}$ and $\tilde{\mathbf{C}}^{(m,n)}$ , $1 \leq m, n \leq M$

## III. AN EFFICIENT IMPLEMENTATION OF ALGEBRAIC DC-CPD

We note that the main complexity of the algebraic DC-CPD algorithm, as it has been presented in the manuscript, is in the construction of the  $(\mathbb{C}_K^2 N^{2K}) \times R^K$  matrices  $\mathbf{T}^{(m,m,\dots,n_K)}$  and the calculation of the basis vectors in their null space. Here we present an efficient way to calculate the basis vectors. In this

implementation, we do not explicitly construct  $\Gamma^{(m,n_1,\dots,n_K)}$ . Instead, we calculate the  $R^K \times R^K$  matrices  $\mathcal{Q}^{(m,n_1,\dots,n_K)} \triangleq \Gamma^{(m,n_1,\dots,n_K)H} \Gamma^{(m,n_1,\dots,n_K)}$ . We note that  $\ker(\mathcal{Q}^{(m,n_1,\dots,n_K)}) = \ker(\Gamma^{(m,n_1,\dots,n_K)})$ , while  $\mathcal{Q}^{(m,n_1,\dots,n_K)}$  have smaller size and can be computed in a more efficient way than  $\Gamma^{(m,n_1,\dots,n_K)}$ , as will be explained later. Hence, in an efficient implementation we use  $\mathcal{Q}^{(m,n_1,\dots,n_K)}$  instead of  $\Gamma^{(m,n_1,\dots,n_K)}$ .

We first explain the simplest case where  $K=2$ . For each  $m, p, q$ , we denote  $\mathcal{Q}^{(m,p,q)} = \Gamma^{(m,p,q)H} \Gamma^{(m,p,q)}$ , where  $\Gamma^{(m,p,q)}$  holds  $\Psi(\mathbf{T}_{(:,s)}^{(m,p)}, \mathbf{T}_{(:,u)}^{(m,q)})$  as its columns. According to (15) in the manuscript, the entries of  $\mathcal{Q}^{(m,p,q)}$  have the form:

$$\begin{aligned} [\mathcal{Q}^{(m,p,q)}]_{(s-1)R+u, (s'-1)R+u'} &= \Psi^H(\mathbf{T}_{(:,s)}^{(m,p)}, \mathbf{T}_{(:,u)}^{(m,q)}) \Psi(\mathbf{T}_{(:,s')}^{(m,p)}, \mathbf{T}_{(:,u')}^{(m,q)}) \\ &= 2 \left( \mathbf{t}_s^{(m,p)H} \mathbf{t}_{s'}^{(m,p)} \right) \left( \mathbf{t}_u^{(m,q)H} \mathbf{t}_{u'}^{(m,q)} \right) \\ &\quad - \sum_{g,h} \left[ \left( \mathbf{t}_{g,s}^{(m,p)H} \mathbf{t}_{h,s'}^{(m,p)} \right) \left( \mathbf{t}_{h,u}^{(m,q)H} \mathbf{t}_{g,u'}^{(m,q)} \right) \right. \\ &\quad \left. + \left( \mathbf{t}_{h,s}^{(m,p)H} \mathbf{t}_{g,s'}^{(m,p)} \right) \left( \mathbf{t}_{g,u}^{(m,q)H} \mathbf{t}_{h,u'}^{(m,q)} \right) \right], \end{aligned} \quad (S15)$$

where vectors  $\mathbf{t}_r^{(m,l)} = \text{vec}(\mathbf{T}_{(:,r)}^{(m,l)})$  have length  $N^2$ , and vectors  $\mathbf{t}_{k,r}^{(m,l)} = \mathbf{T}_{(k,:,r)}^{(m,l)}$  have length  $N$ ,  $l \in \{p, q\}, r \in \{s, s', u, u'\}, k \in \{g, h\}$ . We construct two  $R \times R$  Hermitian matrices  $\mathbf{Z}^{(m,l)} \triangleq \mathbf{T}_3^{(m,l)H} \mathbf{T}_3^{(m,l)}$ , where  $\mathbf{T}_3^{(m,l)}$  is the mode-3 representation of tensor  $\mathcal{T}^{(m,l)}$ . By definition we have:  $\mathbf{Z}^{(m,l)}(s, s') = \mathbf{t}_s^{(m,l)H} \mathbf{t}_{s'}^{(m,l)}$ . In addition, we construct  $NR \times NR$  Hermitian matrices  $\mathbf{Y}^{(m,l)} = \mathbf{T}_2^{(m,l)} \mathbf{T}_2^{(m,l)H}$ , where  $l \in \{p, q\}$ . Index permutation yields  $R^2 \times R^2$  matrices  $\mathbf{Y}_1^{(m,l)}$  and  $\mathbf{Y}_2^{(m,l)}$ :

$$\begin{aligned} [\mathbf{Y}_1^{(m,l)}]_{(s-1)R+s', (i-1)N+j} &= [\mathbf{Y}^{(m,l)}]_{(j-1)R+s', (i-1)R+s}, \\ [\mathbf{Y}_2^{(m,l)}]_{(s-1)R+s', (j-1)N+i} &= [\mathbf{Y}^{(m,l)}]_{(j-1)R+s', (i-1)R+s}. \end{aligned} \quad (S16)$$

Then by definition we know:

$$\begin{aligned} (\mathcal{Q}^{(m,p,q)})_{(s-1)R+u, (s'-1)R+u'} &= 2 \left( \mathbf{Z}^{(m,p)} \right)_{s,s'} \left( \mathbf{Z}^{(m,q)} \right)_{u,u'} \\ &\quad - \left( \mathbf{Y}_1^{(m,p)} \mathbf{Y}_2^{(m,q)T} + \mathbf{Y}_2^{(m,p)} \mathbf{Y}_1^{(m,q)T} \right)_{(s-1)R+s', (u-1)R+u'}. \end{aligned} \quad (S17)$$

In practice, we will precompute  $\mathbf{Z}^{(m,l)}$ ,  $\mathbf{Y}^{(m,l)}$ , and construct Hermitian  $R^2 \times R^2$  matrices  $\mathcal{Q}^{(m,p,q)}$  according to (S16) and (S17). The complexity of computing a single Hermitian matrix  $\mathbf{Z}^{(m,l)}$  is  $O(0.5N^2R^2)$  flops, and the complexity of computing a single Hermitian matrix  $\mathbf{Y}^{(m,l)}$  is  $O(0.5N^3R^2)$  flops. The additional complexity of computing a single Hermitian matrix  $\mathcal{Q}^{(m,p,q)}$  by (S17) is  $O(0.5R^4 + 0.5N^2R^4)$  flops. If we compute the basis vectors of  $\ker(\mathcal{Q}^{(m,p,q)})$  by modified Gram-Schmidt orthogonalization, then the computational cost is  $O(2R^6)$  flops. If we use EVD, then the computational cost is  $O(6R^6)$  flops.

For the indices  $m, l=1, \dots, M, 1 \leq p < q \leq M$ , the algebraic DC-CPD overall requires the construction of  $M^2$  matrices  $\mathbf{Z}^{(m,l)}$  of size  $R \times R$ ,  $M^2$  matrices  $\mathbf{Y}^{(m,l)}$  of size  $NR \times NR$ ,  $MC_M^2$  matrices  $\mathcal{Q}^{(m,p,q)}$  of size  $R^2 \times R^2$ , and the calculation of the  $R$  basis vectors of  $\ker(\mathcal{Q}^{(m,p,q)})$ . The overall complexity is  $O(0.5M^2N^2R^2 + 0.5M^2N^3R^2 + 0.25M^3R^4 + 0.25M^3N^2R^4 + M^3R^6)$  flops. For the memory requirements we consider the storage of the matrices  $\mathbf{Z}^{(m,l)}$ ,  $\mathbf{Y}^{(m,l)}$ ,  $\mathcal{Q}^{(m,p,q)}$ , and the tensors

$\mathcal{W}^{(m,p,q)}$  of size  $R \times R \times R$  (18). We need to store  $O(M^2R^2 + M^2N^2R^2 + 0.5M^3R^4 + 0.5M^3R^3)$  complex numbers. The above expressions for complexity and memory requirements can be simplified to  $O(0.5M^3N^2R^4 + M^3R^6)$  flops and  $O(M^2N^2R^2 + 0.5M^3R^4)$  complex numbers, respectively.

In the general case  $K \in [2, M]$ , we work analogously to the simplest case  $K=2$ . More precisely, for each  $m, n_1, \dots, n_K$ , we denote  $\mathcal{Q}^{(m,n_1,\dots,n_K)} = \Gamma^{(m,n_1,\dots,n_K)H} \Gamma^{(m,n_1,\dots,n_K)}$ , where  $\Gamma^{(m,n_1,\dots,n_K)}$  holds  $\Psi(\mathbf{T}_{(:,s_1)}^{(m,n_1)}, \dots, \mathbf{T}_{(:,s_K)}^{(m,n_K)})$  as its columns. We can express  $\mathcal{Q}^{(m,n_1,\dots,n_K)}$  as:

$$\mathcal{Q}^{(m,n_1,\dots,n_K)} = \sum_{v,w} \mathcal{Q}_{(v,w)}^{(m,n_1,\dots,n_K)}, \quad (S18)$$

where

$$\left( \mathcal{Q}_{(v,w)}^{(m,n_1,\dots,n_K)} \right)_{\tilde{s}, \tilde{u}} = \Psi_{(v,w)}^H(\mathbf{T}_{(:,s_1)}^{(m,n_1)}, \dots, \mathbf{T}_{(:,s_K)}^{(m,n_K)}) \Psi_{(v,w)}(\mathbf{T}_{(:,u_1)}^{(m,n_1)}, \dots, \mathbf{T}_{(:,u_K)}^{(m,n_K)}), \quad (S19)$$

where  $\tilde{s} = \sum_{k=1}^{K-1} (s_k - 1)R^{K-k-1} + 1$ ,  $\tilde{u} = \sum_{k=1}^{K-1} (u_k - 1)R^{K-k-1} + 1$ , and  $\Psi_{(v,w)}(\cdot)$  is the vector representation of  $\Phi_{(v,w)}(\cdot)$  defined in (12). According to (12) and (13) in the manuscript, we have:

$$\begin{aligned} \left( \mathcal{Q}_{(v,w)}^{(m,n_1,\dots,n_K)} \right)_{\tilde{s}, \tilde{u}} &= 2 \prod_{l=1}^K \mathbf{t}_{s_l}^{(m,n_l)H} \mathbf{t}_{u_l}^{(m,n_l)} - \left( \prod_{l \in \{v,w\}} \mathbf{t}_{s_l}^{(m,n_l)H} \mathbf{t}_{u_l}^{(m,n_l)} \right) \\ &\quad \cdot \sum_{g,h} \left[ \left( \mathbf{t}_{g,s_v}^{(m,n_v)H} \mathbf{t}_{h,u_v}^{(m,n_v)} \right) \left( \mathbf{t}_{h,s_w}^{(m,n_w)H} \mathbf{t}_{g,u_w}^{(m,n_w)} \right) \right. \\ &\quad \left. + \left( \mathbf{t}_{h,s_v}^{(m,n_v)H} \mathbf{t}_{g,u_v}^{(m,n_v)} \right) \left( \mathbf{t}_{g,s_w}^{(m,n_w)H} \mathbf{t}_{h,u_w}^{(m,n_w)} \right) \right], \end{aligned} \quad (S20)$$

where vectors  $\mathbf{t}_r^{(m,n_l)} = \text{vec}(\mathbf{T}_{(:,r)}^{(m,n_l)})$  have length  $N^2$ , and vectors  $\mathbf{t}_{k,r}^{(m,n_l)} = \mathbf{T}_{(k,:,r)}^{(m,n_l)}$  have length  $N$ ,  $l=1, \dots, K, k \in \{g, h\}, r \in \{s_1, \dots, s_K, u_1, \dots, u_K\}$ . We construct  $R \times R$  Hermitian matrices  $\mathbf{Z}^{(m,n_l)} \triangleq \mathbf{T}_3^{(m,n_l)H} \mathbf{T}_3^{(m,n_l)}$ , and  $NR \times NR$  Hermitian matrices  $\mathbf{Y}^{(m,n_l)} = \mathbf{T}_2^{(m,n_l)} \mathbf{T}_2^{(m,n_l)H}$ , where  $i \in \{v, w\}$ . Index permutation yields the following matrices:

$$\begin{aligned} [\mathbf{Y}_1^{(m,n_i)}]_{(s_i-1)R+u_i, (g-1)N+h} &= [\mathbf{Y}^{(m,n_i)}]_{(h-1)R+u_i, (g-1)R+s_i}, \\ [\mathbf{Y}_2^{(m,n_i)}]_{(s_i-1)R+u_i, (h-1)N+g} &= [\mathbf{Y}^{(m,n_i)}]_{(h-1)R+u_i, (g-1)R+s_i}. \end{aligned} \quad (S21)$$

Then we have:

$$\begin{aligned} \left( \mathcal{Q}_{(v,w)}^{(m,n_1,\dots,n_K)} \right)_{\tilde{s}, \tilde{u}} &= 2 \prod_{l=1}^K \left( \mathbf{Z}^{(m,n_l)} \right)_{s_l, u_l} - \prod_{l \in \{v,w\}} \left( \mathbf{Z}^{(m,n_l)} \right)_{s_l, u_l} \\ &\quad \cdot \left( \mathbf{Y}_1^{(m,n_v)} \mathbf{Y}_2^{(m,n_w)T} + \mathbf{Y}_2^{(m,n_v)} \mathbf{Y}_1^{(m,n_w)T} \right)_{(s_v-1)R+u_v, (s_w-1)R+u_w}. \end{aligned} \quad (S22)$$

Therefore, we could precompute  $\mathbf{Z}^{(m,n_l)}$  and  $\mathbf{Y}^{(m,n_l)}$ , where  $l=1, \dots, K, i \in \{v, w\}$ , and construct Hermitian  $R^K \times R^K$  matrices  $\mathcal{Q}_{(v,w)}^{(m,n_1,\dots,n_K)}$  according to (S22). The additional complexity of computing a single Hermitian matrix  $\mathcal{Q}_{(v,w)}^{(m,n_1,\dots,n_K)}$  by (S22) is  $O(0.5R^{2K} + 0.5N^2R^{2K})$  flops. To compute  $\mathcal{Q}_{(v,w)}^{(m,n_1,\dots,n_K)}$ , we need to construct  $C_k^2$  matrices  $\mathcal{Q}_{(v,w)}^{(m,n_1,\dots,n_K)}$ , and thus the complexity of computing a single Hermitian matrix  $\mathcal{Q}_{(v,w)}^{(m,n_1,\dots,n_K)}$  is  $O(0.5C_k^2R^{2K} + 0.5C_k^2N^2R^{2K})$ . The complexity of finding the basis vectors of  $\ker(\mathcal{Q}_{(v,w)}^{(m,n_1,\dots,n_K)})$  is  $O(2R^{3K})$  if they are computed by modified Gram-Schmidt orthogonalization. If we use EVD, then the computational cost is  $O(6R^{3K})$  flops.

For the indices  $m=1, \dots, M, 1 \leq n_1 < \dots < n_K \leq M$ , the algebraic DC-CPD overall requires the construction of  $M^2$

matrices  $\mathbf{Z}^{(m,l)}$  of size  $R \times R$ ,  $M^2$  matrices  $\mathbf{Y}^{(m,l)}$  of size  $NR \times NR$ ,  $MC_M^K$  matrices  $\mathbf{Q}^{(m,n,\dots,n_K)}$  of size  $R^K \times R^K$ , and the calculation of the  $R$  basis vectors of  $\ker(\mathbf{Q}^{(m,n,\dots,n_K)})$ . The overall complexity is  $O(0.5M^2N^2R^2 + 0.5M^2N^3R^2 + 0.5MC_M^KC_K^2R^{2K} + 0.5MC_M^KC_K^2N^2R^{2K} + 2MC_M^KR^{3K})$  flops. For the memory requirements we consider the storage of the matrices  $\mathbf{Z}^{(m,l)}$ ,  $\mathbf{Y}^{(m,l)}$ ,  $\mathbf{Q}^{(m,n,\dots,n_K)}$ , and the tensors  $\mathbf{W}^{(m,n,\dots,n_K)}$  of size  $R \times \dots \times R$  (26). Hence, we need to store  $O(M^2R^2 + M^2N^2R^2 + MC_M^KR^{2K} + MC_M^KR^{K+1})$  complex numbers. The above expressions for complexity and memory requirements can be simplified to  $O(0.5MC_M^KC_K^2N^2R^{2K} + 2MC_M^KR^{3K})$  flops and  $O(M^2N^2R^2 + MC_M^KR^{2K})$  complex numbers, respectively.

#### IV. RESULTS OF EXPERIMENT B

Besides the three plots in the manuscript, we provide more results for experiment B, in Fig.1. The plots concern the following three cases: (a) overdetermined J-BSS:  $N = 3, R = 3$ ; (b) slightly underdetermined J-BSS:  $N = 3, R = 4$ ; (c) highly underdetermined J-BSS:  $N = 4, R = 8$ . In each case, parameters such as  $L, T, M$  are varied. With more results for different parameters, we aim to: (a) provide a more comprehensive comparison of the algorithms, and (b) provide insights into how the performance of different methods depends on the parameters. Please refer to the manuscript for the details of the data generation, and the settings for the compared algorithms. For convenience, we put the three plots in the manuscript in the first row of Fig.1, which are renumbered as subfigure (1.1), (1.2), and (1.3), respectively.

From the subfigures, we first draw a few general conclusions about the relative performance of the different algorithms. In the overdetermined case, with subfigures (1.1), (2.1), (3.1), we see that the three DC-CPD algorithms perform better than CPD-C and SOBIUM. GOJD has the best performance at high SNR, and poorer performance than DC-CPD at low SNR. This behavior is consistent for different parameters, and the good performance of GOJD at high SNR is mainly because of the prewhitening step used in this algorithm. M-CCA always performs poorly, because it does not make use of the temporal structure of the signals. Comparing the three DC-CPD algorithms, we note that the results of DC-CPD-ALG are not much improved by the other two optimization based algorithms. This is because in the overdetermined case, the coupled rank-1 detection mapping is not used, and DC-CPD-ALG is close to optimal. Note that the improvement by the optimization based DC-CPD algorithms is more significant in the more challenging underdetermined cases.

In the underdetermined cases, we consistently observe that the DC-CPD algorithms perform better than SOBIUM and CPD-C. The comparison between DC-CPD and SOBIUM and CPD-C, in both overdetermined and underdetermined cases, shows that it is in general advantageous to take more of the

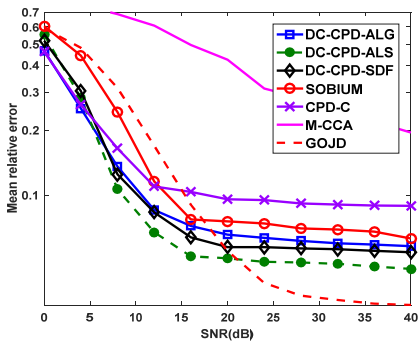
coupling structure into account. The difference between DC-CPD and SOBIUM and CPD-C is more pronounced in cases that are more difficult. Comparing the three DC-CPD algorithms, we see that DC-CPD-ALS has the best performance, followed respectively by DC-CPD-SDF and DC-CPD-ALG. The above general observations are consistent with those reported in the manuscript.

Now we examine how the attained accuracy depends on the choice of parameter values. In the overdetermined case, we note that in comparison with subfigure (1.1), the performance is improved by increasing either the frame length  $L$  or the number of frames  $T$ , as shown in subfigure (2.1) and (3.1), but the improvement is not as much as in the underdetermined case. This is because the overdetermined problem is relatively easy and less sensitive to noise and finite sampling errors. The compared algorithms perform well in general, even if the frame length is very small (note that  $L = 50$  in subfigure (1.1)).

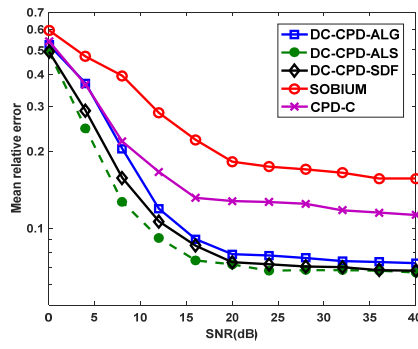
On the other hand, in the highly underdetermined case, with subfigures (1.3), (2.3) and (3.3), the problem itself becomes very sensitive to noise and finite sampling errors. In particular, when  $L = 250, T = 19, M = 3$ , as shown in subfigure (2.3), most of the compared algorithms do not generate reasonable results even at high SNR. When  $L = 250, T = 39, M = 3$ , as shown in subfigure (1.3), the results of the DC-CPD algorithms are reasonably accurate at high SNR. CPD-C and SOBIUM, on the other hand, perform poorly at all SNR levels. The estimation error for all the algorithms decreases monotonically as SNR increases. However, when SNR exceeds 20dB, the increase of SNR does not improve the performance any more. At this point, the accuracy is bounded by the finite sampling errors. When  $L = 1000, T = 79, M = 4$ , as shown in subfigure (3.3), all the compared algorithms perform well at high SNR. The DC-CPD algorithms even generate very accurate results (mean relative error  $< 0.1$ ) at a medium level of SNR (e.g. 10dB). However, this requires a large number of samples (note that in this setting the total number of samples equals 40000). The observations generally illustrate that the highly underdetermined problem is by itself very sensitive to noise and finite sampling errors.

In the slightly underdetermined case, we observe that all the compared algorithms are able to generate reasonably accurate results for medium level of SNR, and medium values of  $L$  and  $T$ , as shown in subfigures (1.2), (2.2), and (4.2). Comparing subfigures (3.2) and (4.1), we see that the decrease of  $T$  results in a large deterioration of the accuracy. In particular, in subfigure (3.2), DC-CPD performs well, while SOBIUM and CPD-C fail to generate the correct results. In subfigure (4.1), none of the algorithms yields good results. In addition, comparing subfigures (1.2), (2.2) and (4.2), we note that the increase of  $L$  improves the performance of all the compared algorithms.

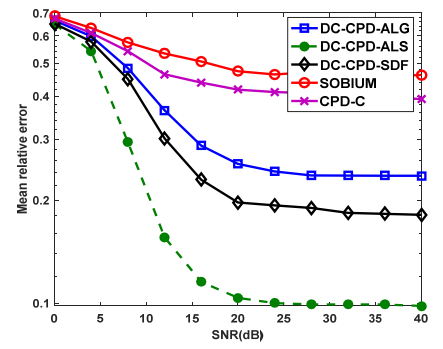




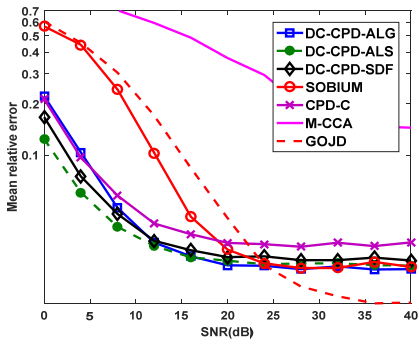
(1.1)  $N = 3, R = 3, M = 3, L = 50, T = 39$



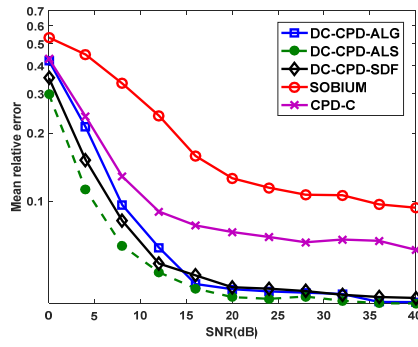
(1.2)  $N = 3, R = 4, M = 3, L = 100, T = 39$



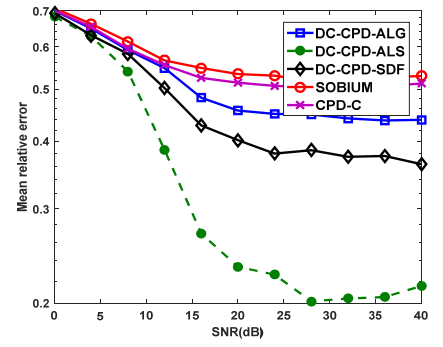
(1.3)  $N = 4, R = 8, M = 3, L = 250, T = 39$



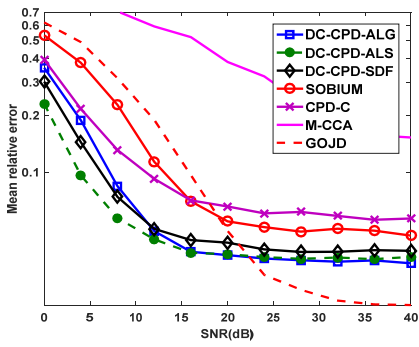
(2.1)  $N = 3, R = 3, M = 3, L = 250, T = 39$



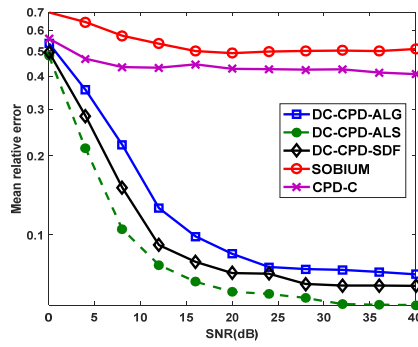
(2.2)  $N = 3, R = 4, M = 3, L = 250, T = 39$



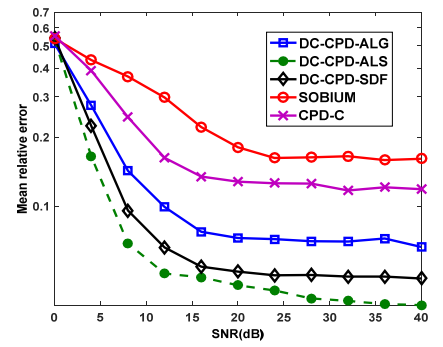
(2.3)  $N = 4, R = 8, M = 3, L = 250, T = 19$



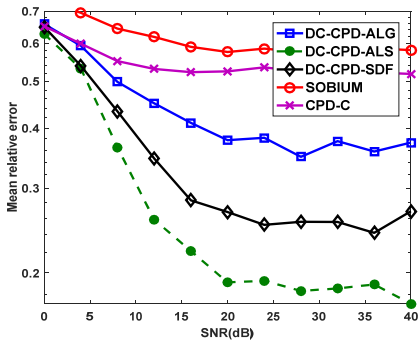
(3.1)  $N = 3, R = 3, M = 3, L = 250, T = 19$



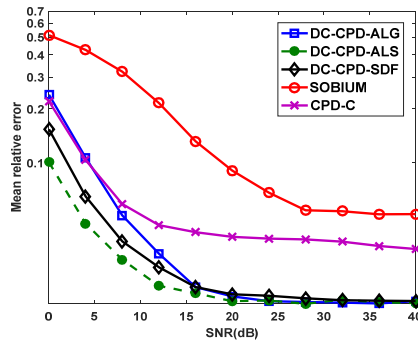
(3.2)  $N = 3, R = 4, M = 3, L = 250, T = 19$



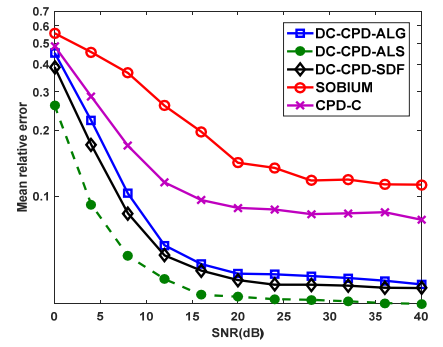
(3.3)  $N = 4, R = 8, M = 4, L = 1000, T = 79$



(4.1)  $N = 3, R = 4, M = 3, L = 250, T = 7$



(4.2)  $N = 3, R = 4, M = 3, L = 1000, T = 39$



(4.3)  $N = 3, R = 4, M = 5, L = 250, T = 39$

Fig. 1. Mean relative error of DC-CPD-ALG, DC-CPD-ALS, DC-CPD-SDF, SOBIUM, and CPD-C vs. SNR in experiment B, in setting (a) M-CCA and GOJD are also included in the comparison. The plots illustrate the performance in (a) an overdetermined setting, (b) a slightly underdetermined setting, and (c) a highly underdetermined setting.

REFERENCES

- [1] M. Sorensen, L. De Lathauwer, “Coupled canonical polyadic decompositions and (coupled) decompositions in multilinear rank- $(L_{r,n}, L_{r,m}, 1)$  terms—Part I: uniqueness,” *SIAM J. Matrix Anal. Appl.*, vol. 36, no. 2, pp. 496–522, May 2015.
- [2] L. De Lathauwer, B. De Moor, J. Vandewalle, “On the best rank-1 and rank- $(R_1, R_2, \dots, R_N)$  approximation of higher-order tensors,” *SIAM J. Matrix Anal. Appl.*, vol. 21, no. 4, pp. 1324–1342, May 2000.
- [3] M. Rajih, P. Comon, R. A. Harshman, “Enhanced line search: a novel method to accelerate PARAFAC,” *SIAM J. Matrix Anal. Appl.*, vol. 30, no. 3, pp. 1128–1147, Sep. 2008.
- [4] D. Nion, L. De Lathauwer, “An enhanced line search scheme for complex-valued tensor decompositions. Application in DS-CDMA,” *Signal Process.*, vol. 88, no. 3, pp. 749–755, Mar. 2008.
- [5] L. Sorber, I. Domanov, M. Van Barel, L. De Lathauwer, “Exact line and plane search for tensor optimization,” *Comput. Optim. Appl.*, pp. 1–22, May 2015.